

Subspace Phase Retrieval

Mengchu Xu, Dekuan Dong and Jian Wang

School of Data Science, Fudan University, Shanghai 200433, China

E-mail: jian_wang@fudan.edu.cn

Abstract—In this paper, we propose a novel algorithm, termed Subspace Phase Retrieval (SPR), which can accurately recover any n -dimensional k -sparse signal from $\mathcal{O}(k \log n)$ magnitude-only Gaussian samples. This offers a significant improvement over some existing results that require $\mathcal{O}(k^2 \log n)$ samples. We also present a geometrical analysis for a subproblem, where we recover the sparse signal given that at least one support index of this signal is identified already. It is shown that with high probability, $\mathcal{O}(k \log k)$ magnitude-only Gaussian samples ensure i) that all local minima of our objective function are clustered around the expected global minimum within arbitrarily small distances, and ii) that all critical points outside of this region have at least one negative curvature. When the input signal is nonsparse (i.e., $k = n$), our result indicates an analogous geometric property with $\mathcal{O}(n \log n)$ samples. This affirmatively answers the open question by Sun-Qu-Wright [1].

Index Terms—Phase retrieval, information-theoretic bound, nonconvex optimization, sparsity, support index.

I. INTRODUCTION

PHASE retrieval arises in dozens of optical imaging applications, such as X-ray imaging, crystallography, coherent diffraction imaging, and atmospheric imaging [2]–[6]. The goal of phase retrieval is to reconstruct a signal $\mathbf{x} \in \mathbb{C}^n$ from its phaseless samples:

$$y_i = |\mathbf{a}_i^* \mathbf{x}|, \quad i = 1, 2, \dots, m, \quad (1)$$

where $\mathbf{a}_i \in \mathbb{C}^m$, $i = 1, \dots, m$, are sampling vectors, such as the discrete Fourier transform basis. In general, the signal reconstruction process involves the following nonconvex optimization problem [7]:

$$\min_{\mathbf{x} \in \mathbb{C}^n} \frac{1}{2m} \sum_{i=1}^m (y_i^2 - |\mathbf{a}_i^* \mathbf{x}|^2)^2. \quad (2)$$

Over the years, much effort has been made to find out the optimal solution for this problem. Gerchberg and Saxton first proposed the GS algorithm [8], which alternates the projections between the image and Fourier domains for error reduction. Fienup suggested a refined version of GS called the hybrid-input output (HIO) algorithm [9]. Although these methods can reconstruct the original signal effectively, they suffer from many drawbacks, such as slow convergence, requiring strong priors (e.g., knowing the support of input signal in advance), and lack of theoretical guarantee [10].

Convex optimization-based approaches for phase retrieval usually enjoy rigorous performance guarantees [11]–[14]. PhaseLift rewrites the phaseless samples in (1) in a linear form

(i.e., $y_i^2 = \mathbf{x}^* \mathbf{a}_i \mathbf{a}_i^* \mathbf{x} = \text{Tr}(\mathbf{x}^* \mathbf{a}_i \mathbf{a}_i^* \mathbf{x}) = \text{Tr}(\mathbf{a}_i \mathbf{a}_i^* \mathbf{x} \mathbf{x}^*)$), thus relaxing (2) to a convex optimization problem [11]:

$$\begin{aligned} & \min_{\mathbf{X} \in \mathbb{C}^{n \times n}} \text{Tr}(\mathbf{X}) \\ & \text{s.t.} \quad y_i^2 = \text{Tr}(\mathbf{a}_i \mathbf{a}_i^* \mathbf{X}), \quad i = 1, \dots, m, \\ & \quad \mathbf{X} \succeq 0. \end{aligned} \quad (3)$$

where $\mathbf{X} \doteq \mathbf{x} \mathbf{x}^* \in \mathbb{C}^{n \times n}$ and $\text{Tr}(\cdot)$ denotes the trace of a matrix. It is shown that when \mathbf{a}_i 's are random Gaussian vectors, the PhaseLift algorithm perfectly recovers the original signal provided that [11]

$$m \geq \mathcal{O}(n \log n). \quad (4)$$

However, this algorithm relies on a semi-definite programming (SDP) approach, which could be computationally burdensome for large-scale applications.

Recently, to improve the computational efficiency, gradient descent-based methods have been suggested. A well-known representative is Wirtinger flow (WF) [15]. It has been shown that the WF algorithm with an elaborated initialization can recover the target signal when the number of samples satisfies (4). There are also some powerful variants of WF, such as the reshaped WF (RWF) [16] and truncated WF (TWF) [17]. Compared to those in the convex optimization family, the gradient descent-based methods have demonstrated to be more efficient both in theory and practice.

There has been much evidence [18] that exploiting the sparse prior of input signals can facilitate the phase retrieval. Algorithms in this category include greedy sparse phase retrieval (GESPAR) [19], sparse truncated amplitude flow (SPARTA) [20], sparse WF (SWF) [21], etc., which minimize the ℓ_0 -norm of the signal of interest. It has been shown that SPARTA and SWF recover exactly any k -sparse signal from

$$m \geq \mathcal{O}(k^2 \log n) \quad (5)$$

phaseless Gaussian samples when the minimum nonzero entry of the target \mathbf{x} obeys $|x_i| \geq \mathcal{O}(\frac{\|\mathbf{x}\|_2}{\sqrt{k}})$ [20], [21]. The sampling complexity substantially advances that of WF when $k \ll \sqrt{n}$.

In this paper, with an aim of enhancing the phase retrieval performance and meanwhile optimizing the theoretical guarantee, we propose a novel algorithm called subspace phase retrieval (SPR). The principle behind the SPR algorithm is simple and intuitive. Initialized with a spectral method, it maintains an estimated support (i.e., index set of the nonzero entries in the input signal \mathbf{x}) of size k , while refining this set iteratively with a pruning strategy until convergence. Experimental results on both synthetic and real-world data demonstrate that the proposed SPR method has competitive

results compared to the state-of-the-art ones, especially when the number of samples is small. Our SPR algorithm also has the attractive features of high efficiency and ease of implementation.

Our main conclusion, Theorem 4, states that with high probability, the SPR algorithm recovers the input signal \mathbf{x} correctly if the number of Gaussian samples satisfies

$$m \geq \mathcal{O}(k \log n). \quad (6)$$

Not only does our result outperform those of SPARTA and SWF by a factor of k , but also it is more general since it has no dependence on the magnitudes of nonzero entries in \mathbf{x} . Note that the constraint $|x_i| \geq \mathcal{O}(\frac{\|\mathbf{x}\|_2}{\sqrt{k}})$ [20] in the theoretical guarantee of SPARTA essentially requires \mathbf{x} to be a ‘‘flat’’ signal. In fact, the proposed sampling complexity is optimal in the sense that it attains the information-theoretic bound for the sparse phase retrieval problem [22], [23]. To the best of our knowledge, SPR is the first practical algorithm to provably achieve this fundamental bound.

Our improvement on the sampling complexity is due to two major factors. The first lies in the initialization step. Specifically, existing algorithms including SPARTA and SWF have to initialize carefully a signal estimate close to the truth \mathbf{x} . In their analyses, they often assumed to catch all support indices with the spectral initialization, which is restrictive and is associated with a sampling complexity of $m \geq \mathcal{O}(k^2 \log n)$ [20], [21]. In [24], the authors put forward a new point of view on the spectral method used in SPARTA, and showed that

$$m \geq \mathcal{O}\left(\max\{k \log n, \log^3 n\} \frac{\|\mathbf{x}\|^2}{|x_{\max}|^2}\right) \quad (7)$$

can ensure exact recovery of the support of \mathbf{x} . In the ideal case where $|x_{\max}|$ dominates the power of \mathbf{x} (i.e., when $\frac{\|\mathbf{x}\|^2}{|x_{\max}|^2} = \Omega(1)$), this number of samples can be reduced to $\mathcal{O}(k \log n)$, while in the general case where small nonzero elements of \mathbf{x} are nontrivial (e.g., when \mathbf{x} is a ‘‘flat’’ signal), the result may still be $\mathcal{O}(k^2 \log n)$.

Finding out all support indices has an equivalent problem in sparse principle component analysis (SPCA) [25], [26], for which the information-theoretic sampling complexity is $\mathcal{O}(k \log n)$, but so far no practical algorithm can achieve it [25]. As pointed out in [27], the spectral method actually becomes a bottleneck dominating the sampling complexity of many phase retrieval algorithms. In order to break this bottleneck, we propose to slightly ‘‘weaken’’ the goal of the initialization step. To be specific, instead of catching all support indices or initializing a signal estimate near \mathbf{x} in this step, our SPR algorithm only needs to capture (at least) one support index, which is much easier to achieve. Indeed, this can be guaranteed with high probability when the number of samples satisfies $m \geq \mathcal{O}(k \log n)$ (Theorem 1).

Second, we provide a geometric property for a subproblem, in which we recover the sparse signal given that at least one support index of this signal is identified already (Proposition 2). Our result shows that with high probability, all local minima of our objective function (i.e., a natural least-squares formulation) are clustered around the expected global optimum

TABLE I: SUMMARY OF NOTATIONS

| Notation | Description |
|------------------------------|---|
| $ \cdot $ | absolute value or modulus |
| $\ \cdot\ $ | ℓ_2 -norm |
| $\ \cdot\ _q$ | ℓ_q -norm of $\mathbf{x} \in \mathbb{C}^n$, i.e., $(\sum_{i=1}^n \mathbf{x} ^q)^{1/q}$ |
| $\bar{\mathbf{x}}$ | conjugate of $\mathbf{x} \in \mathbb{C}^n$ |
| \mathbf{x}^* | conjugate transpose of $\mathbf{x} \in \mathbb{C}^n$ |
| x_i | i th entry of $\mathbf{x} \in \mathbb{C}^n$ |
| $\ \mathbf{x}\ _0$ | number of nonzero entries in $\mathbf{x} \in \mathbb{C}^n$ |
| $\text{supp}(\mathbf{x})$ | support set (i.e., index set of non-zero indices) of $\mathbf{x} \in \mathbb{C}^n$ |
| $\mathbf{x}_{\mathcal{T}}$ | keep the elements of \mathbf{x} indexed by \mathcal{T} and others to 0 |
| $\hat{\mathbf{x}}$ | recovered signal |
| a_{ij} | (i, j) th entry of $\mathbf{A} \in \mathbb{C}^{m \times n}$ |
| $\mathbf{A}_{\mathcal{T}}$ | keep all the rows and columns of \mathbf{A} indexed by \mathcal{T} and set others to 0 |
| ∇f | (Wirtinger) gradient |
| $\nabla^2 f$ | (Wirtinger) Hessian |
| $\mathbb{C}^{\mathcal{T}}$ | subspace $\{\mathbf{x} \in \mathbb{C}^n \text{supp}(\mathbf{x}) \subseteq \mathcal{T}\}$ |
| $\mathcal{C}(\mathbf{x}, k)$ | index set of the k largest entries of \mathbf{x} in magnitude |
| $\Im(\mathbf{x})$ | the imaginary part of \mathbf{x} |

with arbitrarily small distances, while all critical points outside of this region have at least one negative curvature when

$$m \geq \mathcal{O}(k \log k). \quad (8)$$

This geometric structure is favorable as it allows the nonconvex subproblem to be globally optimized by efficient iterative methods. Furthermore, if the estimated support contains the whole support of the input signal \mathbf{x} , the estimated signal just equals \mathbf{x} , up to a global phase (Proposition 3).

The benign geometric property plays a vital role in analyzing the non-initial steps of SPR. Interestingly, it allows the SPR algorithm to recover \mathbf{x} exactly using only two iterations with high probability (Theorem 3), which is very efficient. In [1], an analogous geometric property for the case where \mathbf{x} is nonsparse was studied under the condition of $m \geq \mathcal{O}(n \log^3 n)$. Our analysis directly applies to the nonsparse case when $k = n$. In this case, our result indicates that when $m \geq \mathcal{O}(n \log n)$, with high probability, all the local minima are exactly \mathbf{x} up to a global phase, while all the other critical points have at least one negative curvature. This affirmatively answers the open question in [1].

Our approach has a similar flavor to GESPAR [19] in that they both refine an estimated support iteratively through a replacement-type operation. Nevertheless, our greedy principle is sufficiently distinct. In contrast to the GESPAR algorithm that maintains an estimated support by adding and removing one candidate at each iteration through a 2-opt approach, SPR allows multiple candidates to be updated at once using a properly designed pruning strategy. Furthermore, we provide an analysis of the recovery guarantee for SPR, for which there is no counterpart in the GESPAR study.

The rest of this paper is organized as follows. In Section II, we introduce the sparse phase retrieval problem and the proposed SPR algorithm, and present our main results. In Section II-C, we analyze the geometric property for a subproblem of sparse phase retrieval problem, and give the detailed proofs for exact recovery of sparse signals via SPR. Numerical results are illustrated in Section IV. Finally, conclusion remarks are provided in Section V.

II. PHASE RETRIEVAL VIA SUBSPACE PHASE RETRIEVAL

A. Preliminaries

Consider the sparse phase retrieval problem:

$$\begin{aligned} \text{Find } \mathbf{x} \in \mathbb{C}^n \\ \text{s.t. } y_i = |\mathbf{a}_i^* \mathbf{x}|, \quad i = 1, 2, \dots, m, \\ \|\mathbf{x}\|_0 \leq k, \end{aligned} \quad (9)$$

which can be reformulated in a least-squares form [15]:

$$\min_{\mathbf{x} \in \mathbb{C}^n} \frac{1}{2m} \sum_{i=1}^m \left(y_i^2 - |\mathbf{a}_i^* \mathbf{x}|^2 \right)^2 \quad \text{s.t. } \|\mathbf{x}\|_0 \leq k. \quad (10)$$

Due to the nonconvex sparse constraint, however, it requires a combinatorial search over all possible cases of $\text{supp}(\mathbf{x})$, and thus is NP hard. In this paper, we propose to solve \mathbf{x} in a greedy fashion. Before we proceed to the details of our algorithm, we give some useful definitions.

Observe that $f(\mathbf{x}e^{j\phi}) = f(\mathbf{x})$, $\forall \phi$. In other words, $\mathbf{x}e^{j\phi}$ and \mathbf{x} are equivalent solutions to the problem (10). Thus, it is necessary to define the distance between two points in \mathbb{C}^n under such equivalence class. A nature definition on the distance between the point $\mathbf{z} \in \mathbb{C}^n$ and \mathbf{x} is given by

$$\text{dist}(\mathbf{z}, \mathbf{x}) \doteq \min_{\phi \in [0, 2\pi)} \|\mathbf{z} - \mathbf{x}e^{j\phi}\|. \quad (11)$$

For simplicity, define the loss function of problem (10) as:

$$f: \mathbb{C}^n \mapsto \mathbb{R}, \quad f(\mathbf{z}) = \frac{1}{2m} \sum_{i=1}^m (y_i^2 - |\mathbf{a}_i^* \mathbf{z}|^2)^2. \quad (12)$$

The derivative $\nabla f(\mathbf{x})$ does not exist in general since it does not satisfy Cauchy-Riemann equation. In other words, $f(\mathbf{x})$ is not a holomorphic function. Thus, we introduce the Wirtinger derivative:

$$\frac{\partial f}{\partial \mathbf{z}} \doteq \frac{\partial f(\mathbf{z}, \bar{\mathbf{z}})}{\partial \mathbf{z}} = \left[\frac{\partial f(\mathbf{z}, \bar{\mathbf{z}})}{\partial z_1}, \dots, \frac{\partial f(\mathbf{z}, \bar{\mathbf{z}})}{\partial z_n} \right]; \quad (13)$$

$$\frac{\partial f}{\partial \bar{\mathbf{z}}} \doteq \frac{\partial f(\mathbf{z}, \bar{\mathbf{z}})}{\partial \bar{\mathbf{z}}} = \left[\frac{\partial f(\mathbf{z}, \bar{\mathbf{z}})}{\partial \bar{z}_1}, \dots, \frac{\partial f(\mathbf{z}, \bar{\mathbf{z}})}{\partial \bar{z}_n} \right]. \quad (14)$$

The Wirtinger derivative treats f as a binary function of \mathbf{z} and $\bar{\mathbf{z}}$, and compute their derivatives, respectively; see [28] for a comprehensive tutorial of Wirtinger Calculus.

The Wirtinger derivative has been widely adopted to analyze the phase retrieval problem where the input signal is complex [1], [15]. In terms of the Wirtinger derivative, the Wirtinger gradient and Hessian matrix can be given by

$$\nabla f(\mathbf{z}) = \left[\frac{\partial f}{\partial \mathbf{z}}, \frac{\partial f}{\partial \bar{\mathbf{z}}} \right]^* \quad (15)$$

and

$$\nabla^2 f(\mathbf{z}) = \begin{bmatrix} \frac{\partial}{\partial \mathbf{z}} \left(\frac{\partial f}{\partial \mathbf{z}} \right)^* & \frac{\partial}{\partial \bar{\mathbf{z}}} \left(\frac{\partial f}{\partial \mathbf{z}} \right)^* \\ \frac{\partial}{\partial \mathbf{z}} \left(\frac{\partial f}{\partial \bar{\mathbf{z}}} \right)^* & \frac{\partial}{\partial \bar{\mathbf{z}}} \left(\frac{\partial f}{\partial \bar{\mathbf{z}}} \right)^* \end{bmatrix}, \quad (16)$$

respectively. Hereafter, we write

$$\nabla_1 f(\mathbf{z}) = \left(\frac{\partial f}{\partial \mathbf{z}} \right)^* \quad \text{and} \quad \nabla_2 f(\mathbf{z}) = \left(\frac{\partial f}{\partial \bar{\mathbf{z}}} \right)^* \quad (17)$$

for notational convenience. Table I summarizes some notations used throughout this paper.

Algorithm 1 SPECTRAL INITIALIZATION

- 1: **Input:** sparsity k , \mathbf{y} , $\mathbf{A} = \{a_{i,j}\}_{i=1,j=1}^{m \times n}$.
 - 2: Compute $Z_j = \frac{1}{m} \sum_{i=1}^m y_i |a_{i,j}|$.
 - 3: Sort $\{Z_j\}_{j=1}^n$ to generate an index set Λ whose elements correspond to the k largest values of Z_j 's.
 - 4: Generate a length- n zero vector \mathbf{x}^0 and set the elements indexed by Λ to be one.
 - 5: **Output:** \mathbf{x}^0
-

Algorithm 2 SUBSPACE PHASE RETRIEVAL (SPR)

- 1: **Input:** sparsity k , samples \mathbf{y} , sampling matrix \mathbf{A} , tolerance δ , maximal iteration number i_{\max} .
 - 2: **Initialize:** iteration count $i \leftarrow 0$, signal estimate \mathbf{x}^0 with spectral method, estimated support $S^0 \leftarrow \text{supp}(\mathbf{x}^0)$.
 - 3: **while** $i < i_{\max}$ and $f(\mathbf{x}^i) \geq \delta$ **do**
 - 4: $i \leftarrow i + 1$.
 - 5: Matching: $\hat{S}^i \leftarrow S^{i-1} \cup \mathcal{C}(\nabla_1 f(\mathbf{x}^{i-1}), k)$.
 - 6: Projection: $\mathbf{x}^i \leftarrow \arg \min_{\mathbf{z}: \text{supp}(\mathbf{z}) = \hat{S}^i} f(\mathbf{z})$.
 - 7: Pruning: $S^i \leftarrow \mathcal{C}(\mathbf{x}^i, k)$.
 - 8: **end while**
 - 9: **Output:** estimated signal $\hat{\mathbf{x}} = \mathbf{x}_{S^i}^i$.
-

B. The SPR algorithm

Now we are ready to describe the SPR algorithm, which consists of two major steps. In the initialization step, a signal estimate is generated with the spectral method; see Alg. 1. The strategy for generating the initialized support and signal is different from that of SPARTA [20].

In the non-initial step of SPR, three operations are involved.

- i) The first operation is called ‘‘matching’’, in which the Wirtinger gradient $\nabla_1 f(\mathbf{x}^{i-1})$ is computed. Then, the indices corresponding to the maximal k values are chosen as the new elements of the estimated support:

$$\hat{S}^i \leftarrow S^{i-1} \cup \mathcal{C}(\nabla_1 f(\mathbf{x}^{i-1}), k), \quad (18)$$

where $\mathcal{C}(\cdot, k)$ is a function that returns the index set of the largest (in magnitude) k entries.

- ii) In the second operation, a signal estimate is obtained via the following optimization:

$$\mathbf{x}^i \leftarrow \arg \min_{\mathbf{z}: \text{supp}(\mathbf{z}) = \hat{S}^i} f(\mathbf{z}). \quad (19)$$

This is referred to as ‘‘projection’’, which can be viewed as a subproblem of (10). The solution always exists since $f(\mathbf{z}) \geq 0$. We shall show from the theoretical analysis that the geometric property of this subproblem is incredibly sound when the estimated support \hat{S}^i contains at least one support index of \mathbf{x} . Thus, a wide range of iterative algorithms (e.g., the perturbed gradient descent (PGD) [29] and Barzilai-Borwein Method (BB) [30]) can solve \mathbf{x}^i efficiently.

- iii) The third operation, termed ‘‘pruning’’, narrows down the number of candidates in \hat{S}^i to k corresponding to the most significant k entries in the vector \mathbf{x}^i ,

$$S^i \leftarrow \mathcal{C}(\mathbf{x}^i, k). \quad (20)$$

The algorithm refines the estimated support S^i iteratively until some desired criterion is met. The mathematical formulation of SPR is specified in Alg. 2.

Whenever the estimated support \hat{S}^i (of size $2k$) contains the true support of \mathbf{x} (i.e., $\hat{S}^i \supset \text{supp}(\mathbf{x})$), we must have $S^i = \text{supp}(\mathbf{x})$, and thus $\hat{\mathbf{x}} = \mathbf{x}$ up to a global phase. This is also ensured by the geometric property of the subproblem (19), which will be discussed thoroughly in Section II-C.

C. Theoretical Results

To demonstrate the effectiveness of SPR, we analyze the initialization and non-initial steps separately. Here we consider that the sampling matrix \mathbf{A} is generic with independent identically distributed (*i.i.d.*) entries obeying the standard complex Gaussian distribution (i.e., $a_{ij} \stackrel{i.i.d.}{\sim} \mathcal{N}(0, \frac{1}{2}) + j\mathcal{N}(0, \frac{1}{2})$). The following theorem gives a condition that guarantees SPR to catch at least one support index of \mathbf{x} with the spectral initialization.

Theorem 1 (Initialization Step): Consider the sparse phase retrieval problem (10). With probability exceeding $1 - n^{-1}$, SPR initializes a signal estimate whose support contains at least one support index of \mathbf{x} provided that $m \geq Ck \log n$.

We follow the convention that letters c and C , and their indexed versions indicate positive, universal constants that may vary at each appearance.

Next, we proceed to characterize the behavior of SPR in the non-initial step, given that at least one support index was caught previously. However, deriving a guarantee for this step is more difficult. The reason is that the projection operation of SPR in (19) has no closed-form solution, since it solves a nonconvex quartic equation. This is in contrast to the WF algorithm that produces a signal estimate in each iteration with an explicit expression (i.e., the gradient descent form) [15]. Also, our projection operation differs with the conventional least squares projection in the compressed sensing literature, which directly has a pseudo-inverse solution over the estimated support (see, e.g., [31]–[36]). The fact that the projection operation of SPR having no analytical expression has posted a major challenge for evaluating the recovery error theoretically.

To cope with this challenge, we first consider an ideal case where there are infinitely many samples, which is essentially the expectation case. We will show that if at least one support index was caught in the previous iteration (i.e., $S^{i-1} \cup \text{supp}(\mathbf{x}) \neq \emptyset$, $i \geq 1$), then the original signal \mathbf{x} can be recovered correctly within additional two iterations. Our result is formally described in the following theorem.

Theorem 2: Consider the sparse phase retrieval problem (10) with $m \rightarrow \infty$. If the estimated support in the $(i-1)$ th iteration of SPR satisfies $S^{i-1} \cap \text{supp}(\mathbf{x}) \neq \emptyset$, then

$$\mathbf{x}^{i+1} = \mathbf{x}e^{j\phi} \quad (21)$$

for some $\phi \in [0, 2\pi)$.

Then, we will show that SPR does not really need infinite number of samples to ensure the success in the non-initial step. In fact, $m \geq \mathcal{O}(k \log k)$ already suffices.

Theorem 3 (Non-initial Step): Consider the sparse phase retrieval problem (10) with $m \geq Ck \log k$. If the estimated support in the $(i-1)$ th iteration of SPR satisfies $S^{i-1} \cap \text{supp}(\mathbf{x}) \neq \emptyset$, then with probability exceeding $1 - cm^{-1}$,

$$\mathbf{x}^{i+1} = \mathbf{x}e^{j\phi} \quad (22)$$

for some $\phi \in [0, 2\pi)$.

One can interpret from the theorem that as long as the initialization step (i.e., when $i = 1$) catches at least one support index, then the SPR algorithm can recover the input signal exactly from $m \geq \mathcal{O}(k \log n)$ samples within only two iterations. Note that the goal of capturing at least one support index can be readily achieved via a spectral initialization provided that $m \geq \mathcal{O}(k \log n)$, as discussed in Theorem 1. Thus, the proposed SPR algorithm is very efficient.

Combining Theorems 1 and 3 leads immediately to an overall guarantee for the SPR algorithm.

Theorem 4 (Overall Guarantee): Consider the sparse phase retrieval problem (10). If $m \geq Ck \log n$, then with probability exceeding $1 - cm^{-1}$, the SPR algorithm generates a signal estimate satisfying

$$\hat{\mathbf{x}} = \mathbf{x}e^{j\phi} \quad (23)$$

for some $\phi \in [0, 2\pi)$.

III. ANALYSIS

A. Proof of Theorem 1

We first introduce Bernstein's Inequality, which is useful for our analysis.

Lemma 1 (Bernstein's inequality [37, Chap. 2.8]): Let X_1, X_2, \dots, X_m be *i.i.d.* copies of the subexponential variable X with parameter σ^2 , then

$$\begin{aligned} \mathbb{P} \left(\left| \frac{1}{m} \left(\sum_{i=1}^m X_i - \mathbb{E}[X] \right) \right| \leq \epsilon \right) \\ \leq 2 \exp \left(-cm \min \left(\frac{\epsilon^2}{\sigma^2}, \frac{\epsilon}{\sigma} \right) \right). \end{aligned} \quad (24)$$

holds for any positive ϵ , where c is absolute positive constant.

Now we present the proof for Theorem 1.

Proof. Denote $Z_{i,j} = |\mathbf{a}_i^* \mathbf{x}| |a_{i,j}|$. We can view $\mathbf{a}_i^* \mathbf{x}$ and $a_{i,j}$ as the random variables at time 0 and τ of a complex Gaussian process, respectively. According to [38, Chap. 2.1.4], the expectation of $Z_{i,j}$ is equivalent to the auto-correlation of the envelope of the complex Gaussian process. Thus, by following the result in [38, Eq. (2.72)], we have

$$\begin{aligned} \mathbb{E}[Z_{i,j}] &= \frac{\pi}{4} \|\mathbf{x}\| F \left(-\frac{1}{2}, -\frac{1}{2}; 1; \frac{|x_j|^2}{\|\mathbf{x}\|^2} \right) \\ &= \frac{\pi}{4} \|\mathbf{x}\| \left(1 + \frac{1}{4} \frac{|x_j|^2}{\|\mathbf{x}\|^2} + \frac{1}{64} \frac{|x_j|^4}{\|\mathbf{x}\|^4} + \dots \right) \\ &\geq \frac{\pi}{4} \|\mathbf{x}\| \left(1 + \frac{1}{4} \frac{|x_j|^2}{\|\mathbf{x}\|^2} \right) \end{aligned} \quad (25)$$

where $F(a, b; c; z)$ is the hypergeometric function defined for $|z| < 1$ by the power series:

$$\begin{aligned} F(a, b; c; z) &= \sum_{i=0}^{\infty} \frac{(a)_i (b)_i}{(c)_i} \frac{z^i}{i!} \\ &= 1 + \frac{ab}{c} \frac{z}{1!} + \frac{a(a+1)b(b+1)}{c(c+1)} \frac{z^2}{2!} + \dots \end{aligned}$$

Hence,¹

$$\begin{cases} \mathbb{E}[Z_{i,j}] = \frac{\pi}{4} \|\mathbf{x}\|, & \text{if } j \notin \text{supp}(\mathbf{x}), \\ \mathbb{E}[Z_{i,j}] \geq \frac{\pi}{4} \|\mathbf{x}\| + \frac{\pi}{16} \frac{|x_j|^2}{\|\mathbf{x}\|}, & \text{if } j \in \text{supp}(\mathbf{x}). \end{cases} \quad (26)$$

In the following, we derive a condition that guarantee the spectral initialization of SPR to catch at least one support index. Since SPR chooses the set Λ of k indices corresponding to the maximum k values of Z_j 's, we must have

$$\frac{1}{k} \sum_{j \in \Lambda} Z_j \geq \frac{1}{k} \sum_{j \in \text{supp}(\mathbf{x})} Z_j. \quad (27)$$

For simplicity, we define

$$\begin{cases} V_i = \frac{1}{k} \sum_{j \in \text{supp}(\mathbf{x})} Z_{i,j}, \\ U_i = \frac{1}{k} \sum_{j \in \Lambda} Z_{i,j}. \end{cases} \quad (28)$$

It is obvious that $\frac{1}{m} \sum_{i=1}^m V_i = \frac{1}{k} \sum_{j \in \text{supp}(\mathbf{x})} Z_j$ and $\frac{1}{m} \sum_{i=1}^m U_i = \frac{1}{k} \sum_{j \in \Lambda} Z_j$. So, (27) can be rewritten as

$$\frac{1}{m} \sum_{i=1}^m U_i \geq \frac{1}{m} \sum_{i=1}^m V_i. \quad (29)$$

Then, we show by contradiction that Λ contains at least one element in $\text{supp}(\mathbf{x})$.

- On the one hand, we obtain from (26) that

$$\mathbb{E}[V_i] \geq \left(\frac{\pi}{4} + \frac{\pi}{16k} \right) \|\mathbf{x}\|. \quad (30)$$

Note that $V_i = |\mathbf{a}_i^* \mathbf{x}| \left(\frac{1}{k} \sum_{j \in \text{supp}(\mathbf{x})} |a_{i,j}| \right)$. It is easily verified that $|\mathbf{a}_i^* \mathbf{x}|$ is a subgaussian variable with parameter $\|\mathbf{x}\|^2$ and that $\frac{1}{k} \sum_{j \in \text{supp}(\mathbf{x})} |a_{i,j}|$ is the sum of k independent subgaussian variables with parameter $\frac{1}{k}$. Thus, V_i is the product of two subgaussian variables, which is subexponential with parameter less than $\frac{\|\mathbf{x}\|^2}{k}$ [37, Lemma 2.7.7]. Applying Bernstein's inequality in Lemma 1 yields the tail bound

$$\begin{aligned} \mathbb{P} \left(\frac{1}{m} \sum_{i=1}^m V_i \leq \mathbb{E}[V_i] - \epsilon \right) \\ \leq \exp \left(-c_1 m \min \left(\frac{k\epsilon^2}{\|\mathbf{x}\|^2}, \frac{\sqrt{k}\epsilon}{\|\mathbf{x}\|} \right) \right), \end{aligned} \quad (31)$$

where c_1 is an absolute positive constant. Using (30) and taking $\epsilon = \frac{\pi}{32k} \|\mathbf{x}\|$, we further have

$$\mathbb{P} \left(\frac{1}{m} \sum_{i=1}^m V_i \leq \left(\frac{\pi}{4} + \frac{\pi}{32k} \right) \|\mathbf{x}\| \right) \leq \exp \left(-\frac{c_1 m}{k} \right).$$

¹If all quantities are real, the coefficients will change slightly, as shown in [39]. To be specific, $\pi/4$ will become $2/\pi$ and $\pi/16$ will become $1/6$. In essence, these minor changes will not influence our proof.

Therefore, when $m \geq (c_1 + 1)k \log n \geq c_1 k \log(2n)$, it holds with probability exceeding $1 - \frac{1}{2n}$ that

$$\frac{1}{m} \sum_{i=1}^m V_i > \left(\frac{\pi}{4} + \frac{\pi}{32k} \right) \|\mathbf{x}\|. \quad (32)$$

- On the other hand, if $\Lambda \cap \text{supp}(\mathbf{x}) = \emptyset$, we obtain from (26) that

$$\mathbb{E}[U_i] = \frac{\pi}{4} \|\mathbf{x}\|. \quad (33)$$

Similarly, we can show that U_i is also subexponential with parameter $\frac{\|\mathbf{x}\|^2}{k}$. Then, applying Bernstein's inequality produces the tail bound

$$\begin{aligned} \mathbb{P} \left(\frac{1}{m} \sum_{i=1}^m U_i \geq \mathbb{E}[U_i] + \epsilon \right) \\ \leq \exp \left(-c_2 m \min \left(\frac{k\epsilon^2}{\|\mathbf{x}\|^2}, \frac{\sqrt{k}\epsilon}{\|\mathbf{x}\|} \right) \right), \end{aligned} \quad (34)$$

where c_2 is an absolute positive constant. By taking $\epsilon = \frac{\pi}{32k} \|\mathbf{x}\|$ and using (33), we have

$$\mathbb{P} \left(\frac{1}{m} \sum_{i=1}^m U_i \geq \left(\frac{\pi}{4} + \frac{\pi}{32k} \right) \|\mathbf{x}\| \right) \leq \exp \left(-\frac{c_2 m}{k} \right).$$

Therefore, when $m \geq (c_2 + 1)k \log n \geq c_2 k \log(2n)$, it holds with probability exceeding $1 - \frac{1}{2n}$ that

$$\frac{1}{m} \sum_{i=1}^m U_i < \left(\frac{\pi}{4} + \frac{\pi}{32k} \right) \|\mathbf{x}\|. \quad (35)$$

By combining (32) and (35), we obtain that with probability exceeding $1 - \frac{1}{n}$,

$$\frac{1}{m} \sum_{i=1}^m U_i < \frac{1}{m} \sum_{i=1}^m V_i, \quad (36)$$

which contradicts with (29). Therefore, with probability exceeding $1 - \frac{1}{n}$, Λ contains at least one support index when $m \geq Ck \log n$. \square

B. Proof of Theorem 2

Before presenting the details of proof, we give some useful observations on the projection operation of SPR in (19). While the projection has no analytical solution in general, we will show from the geometric perspective that obtaining a closed-form solution is still possible in the expectation case, i.e., when there are infinitely many samples.

To begin with, we give the concrete forms of (15) and (16) in (37) and (38), respectively. Then, we obtain that

$$\mathbb{E}[f(\mathbf{z})] = \|\mathbf{x}\|^4 + \|\mathbf{z}\|^4 - \|\mathbf{x}\|^2 \|\mathbf{z}\|^2 - |\mathbf{x}^* \mathbf{z}|^2, \quad (39)$$

$$\nabla_1 \mathbb{E}[f(\mathbf{z})] = ((2\|\mathbf{z}\|^2 - \|\mathbf{x}\|^2) \mathbf{I} - \mathbf{x} \mathbf{x}^*) \mathbf{z}, \quad (40)$$

$$\nabla^2 \mathbb{E}[f(\mathbf{z})] = \begin{bmatrix} \mathbf{B}_{11} & \mathbf{B}_{12} \\ \mathbf{B}_{21} & \mathbf{B}_{22} \end{bmatrix}, \quad (41)$$

$$\nabla f(\mathbf{z}) = \frac{1}{m} \sum_{i=1}^m \left[\begin{array}{c} (|\mathbf{a}_i^* \mathbf{z}|^2 - y_i^2) \mathbf{a}_i \mathbf{a}_i^* \mathbf{z} \\ (|\mathbf{a}_i^* \mathbf{z}|^2 - y_i^2) (\mathbf{a}_i \mathbf{a}_i^*)^\top \bar{\mathbf{z}} \end{array} \right], \quad (37)$$

$$\nabla^2 f(\mathbf{z}) = \frac{1}{m} \sum_{i=1}^m \left[\begin{array}{cc} (2|\mathbf{a}_i^* \mathbf{z}|^2 - y_i^2) \mathbf{a}_i \mathbf{a}_i^* & ((\mathbf{a}_i^* \mathbf{z})^2 \mathbf{a}_i \mathbf{a}_i^\top) \\ ((\mathbf{z}^* \mathbf{a}_i)^2 \bar{\mathbf{a}}_i \mathbf{a}_i^*) & ((2|\mathbf{a}_i^* \mathbf{z}|^2 - y_i^2) \bar{\mathbf{a}}_i \mathbf{a}_i^\top) \end{array} \right]. \quad (38)$$

where

$$\begin{aligned} \mathbf{B}_{11} &= 2\mathbf{z}\mathbf{z}^* - \mathbf{x}\mathbf{x}^* + (2\|\mathbf{z}\|^2 - \|\mathbf{x}\|^2)\mathbf{I}, \\ \mathbf{B}_{12} &= 2\mathbf{z}\mathbf{z}^\top, \\ \mathbf{B}_{21} &= 2\bar{\mathbf{z}}\bar{\mathbf{z}}^*, \\ \mathbf{B}_{22} &= 2\bar{\mathbf{z}}\bar{\mathbf{z}}^\top - \bar{\mathbf{x}}\bar{\mathbf{x}}^\top + (2\|\bar{\mathbf{z}}\|^2 - \|\bar{\mathbf{x}}\|^2)\mathbf{I}. \end{aligned}$$

For the sake of generality, let \mathcal{T} denote the currently estimated support of SPR, over which the projection operation is performed. Also, let $\mathbb{C}^{\mathcal{T}}$ denote the subspace $\{\mathbf{z} \in \mathbb{C}^n \mid \text{supp}(\mathbf{z}) \subseteq \mathcal{T}\}$.

When $m \rightarrow \infty$, the optimization problem (19) can be rewritten as

$$\min_{\mathbf{z}: \text{supp}(\mathbf{z})=\mathcal{T}} \mathbb{E}[f(\mathbf{z})]. \quad (42)$$

Since $\mathbf{z} \in \mathbb{C}^{\mathcal{T}}$, finding out the solution to (42) is equivalent to solving

$$\nabla_1 \mathbb{E}[f(\mathbf{z})]_{\mathcal{T}} = \mathbf{0}. \quad (43)$$

The following proposition characterizes the geometric property of the zero points of $\nabla_1 \mathbb{E}[f(\mathbf{z})]_{\mathcal{T}}$.

Proposition 1: If $\mathcal{T} \cap \text{supp}(\mathbf{x}) \neq \emptyset$, then the zero points of $\nabla_1 \mathbb{E}[f(\mathbf{z})]_{\mathcal{T}}$ belong to the following three classes:

- i) $\mathbf{z} = \mathbf{0}$,
- ii) $\mathbf{z} \in \{\lambda_{\mathcal{T}} \mathbf{x}_{\mathcal{T}} : \lambda_{\mathcal{T}} \in \mathbb{C}, |\lambda_{\mathcal{T}}| = \sqrt{\frac{\|\mathbf{x}\|^2 + \|\mathbf{x}_{\mathcal{T}}\|^2}{2\|\mathbf{x}_{\mathcal{T}}\|^2}}\}$,
- iii) $\mathbf{z} \in \mathcal{S} \doteq \{\mathbf{z} \in \mathbb{C}^{\mathcal{T}} : \mathbf{x}^* \mathbf{z} = 0, \|\mathbf{z}\| = \frac{\|\mathbf{x}\|}{\sqrt{2}}\}$,

which are the local maximum, local minimum, and saddle points of the function $\mathbb{E}[f(\mathbf{z})]$ on the subspace $\mathbb{C}^{\mathcal{T}}$, respectively. Also, local maximum and each saddle point have at least one negative curvature.

One can interpret from this proposition that when $\mathcal{T} \cap \text{supp}(\mathbf{x}) \neq \emptyset$, the subproblem in (19) has a benign geometric property in the expectation sense. In particular, the minimum value of the objective function $\mathbb{E}[f(\mathbf{z})]$ can only be attained at the local minimum $\lambda_{\mathcal{T}} \mathbf{x}_{\mathcal{T}}$ (which is in closed-form). Therefore, $\lambda_{\mathcal{T}} \mathbf{x}_{\mathcal{T}}$ is also the global minimum.

Now we are ready to present the proof of Theorem 2.

Proof. In the i th iteration of SPR, since $S^{i-1} \cap \text{supp}(\mathbf{x}) \neq \emptyset$ and $\hat{S}^i \supseteq S^{i-1}$, we have

$$\hat{S}^i \cap \text{supp}(\mathbf{x}) \neq \emptyset. \quad (44)$$

By applying Proposition 1 with $\mathcal{T} = \hat{S}^i$, we obtain that

$$\mathbf{x}^i = \lambda_{\hat{S}^i} \mathbf{x}_{\hat{S}^i}, \quad (45)$$

which is the solution of the projection operation (i.e., the solution to (42)). Thus,

$$\text{supp}(\mathbf{x}^i) = \text{supp}(\mathbf{x}_{\hat{S}^i}) = \hat{S}^i \cap \text{supp}(\mathbf{x}), \quad (46)$$

which has no more than k indices. Since the pruning operation (i.e., $S^i \leftarrow \mathcal{C}(\mathbf{x}^i, k)$) returns a set of k indices, we have

$$S^i = \hat{S}^i \cap \text{supp}(\mathbf{x}). \quad (47)$$

In the $(i+1)$ th iteration, the matching operation computes

$$\nabla_1 \mathbb{E}[f(\mathbf{x}^i)] = \lambda_{\hat{S}^i} \|\mathbf{x}_{\hat{S}^i}\|^2 (\mathbf{x}_{\hat{S}^i} - \mathbf{x}), \quad (48)$$

and adds a set of k indices to S^i corresponding to the most significant k elements of $\nabla_1 \mathbb{E}[f(\mathbf{x}^i)]$. Since

$$\text{supp}(\nabla_1 \mathbb{E}[f(\mathbf{x}^i)]) = \text{supp}(\mathbf{x}_{\hat{S}^i} - \mathbf{x}) = \text{supp}(\mathbf{x}) \setminus \hat{S}^i \quad (49)$$

has no more than k indices in total, the added index set must include $\text{supp}(\mathbf{x}) \setminus \hat{S}^i$. In other words,

$$\mathcal{C}(\nabla_1 \mathbb{E}[f(\mathbf{x}^i)], k) \supseteq \text{supp}(\mathbf{x}) \setminus \hat{S}^i, \quad (50)$$

which is precisely the remaining elements of $\text{supp}(\mathbf{x})$ that haven't been selected before.

In summary,

$$\begin{aligned} \hat{S}^{i+1} &= S^i \cup \mathcal{C}(\nabla_1 \mathbb{E}[f(\mathbf{x}^i)], k) \\ &\stackrel{(50)}{\supseteq} S^i \cup (\text{supp}(\mathbf{x}) \setminus \hat{S}^i) \\ &\stackrel{(47)}{=} (\text{supp}(\mathbf{x}) \cap \hat{S}^i) \cup (\text{supp}(\mathbf{x}) \setminus \hat{S}^i) \\ &= \text{supp}(\mathbf{x}) \end{aligned} \quad (51)$$

Again, by applying Proposition 1 with $\mathcal{T} = \hat{S}^{i+1} = \text{supp}(\mathbf{x})$, we have $|\lambda_{\hat{S}^{i+1}}| = 1$ and

$$\mathbf{x}^{i+1} = \lambda_{\hat{S}^{i+1}} \mathbf{x}_{\hat{S}^{i+1}} = \mathbf{x} e^{j\phi} \quad (52)$$

for some $\phi \in [0, 2\pi)$. Therefore, the signal recovery is exact in the expectation case. \square

C. Proof of Theorem 3

In Proposition 1, we have analyzed the geometric property of the subproblem (19) in the expectation case (i.e., when $m \rightarrow \infty$). The geometric property is quite favorable and plays a vital role in the proof of Theorem 2. The proof of Theorem 3 also relies on the geometric property of (19), but in the case of finite samples. For this case, exploration of the geometric property is more complex.

First, we explain our main idea for analyzing the geometric property of (19). Recall that \mathcal{T} is the currently estimated support over which the projection operation of SPR is performed. Inspired by Proposition 1, we speculate that when $\mathcal{T} \cap \text{supp}(\mathbf{x}) \neq \emptyset$, the local minima of $f(\mathbf{z})$ are clustered around the expected global minimum $\lambda_{\mathcal{T}} \mathbf{x}_{\mathcal{T}}$ where $\lambda_{\mathcal{T}} \in \mathbb{C}$ and $|\lambda_{\mathcal{T}}| = \sqrt{\frac{\|\mathbf{x}\|^2 + \|\mathbf{x}_{\mathcal{T}}\|^2}{2\|\mathbf{x}_{\mathcal{T}}\|^2}}$, while the critical points outside of this region have at least one negative curvature. If so, the

subproblem (19) also has a favorable geometric property for the case of finite samples.

Before confirming our speculation, we show that the Wirtinger gradient and Hessian matrix of the function $f(\mathbf{z})$ can be well approximated by their expected counterparts.

Lemma 2: If $\mathcal{T} \cap \text{supp}(\mathbf{x}) \neq \emptyset$, then for any constant $\delta > 0$, there exist constants c, C such that when $m \geq Ck \log k$,

$$\|\nabla f(\mathbf{z})_{\mathcal{T}} - \nabla \mathbb{E}[f(\mathbf{z})]_{\mathcal{T}}\| \leq \sqrt{2}\delta \|\mathbf{z}\|(\|\mathbf{x}\|^2 + \|\mathbf{z}\|^2), \quad (53)$$

$$\|\nabla^2 f(\mathbf{z})_{\mathcal{T}} - \nabla^2 \mathbb{E}[f(\mathbf{z})]_{\mathcal{T}}\| \leq \delta(\|\mathbf{x}\|^2 + 3\|\mathbf{z}\|^2) \quad (54)$$

hold for any vector $\mathbf{z} \in \mathbb{C}^{\mathcal{T}}$ with probability at least $1 - cm^{-1}$.

Next, with Lemma 2 in hand, we can safely divide the solution space $\mathbb{C}^{\mathcal{T}}$ of (19) into five regions (i.e., \mathcal{R}_0 – \mathcal{R}_4); see (55)–(59), where $\{\delta_1, \dots, \delta_4\}$ is a set of positive absolute constants, $\mathbf{u} \doteq \lambda_{\mathcal{T}} \mathbf{x}_{\mathcal{T}}$ is defined for notational simplicity, and $\phi(\mathbf{z}) = \arg \min_{\phi \in [0, 2\pi)} \|\mathbf{z} - \mathbf{u}e^{j\phi}\|^2$. For each region, we will discuss the geometric property of (19) separately.

The way we divide the regions is inspired from [1]. Below we give some explanation for these regions.

- i) Observe that the expected global minimum of the function $f(\mathbf{z})$ satisfies

$$\|\lambda_{\mathcal{T}} \mathbf{x}_{\mathcal{T}}\|^2 = \frac{\|\mathbf{x}\|^2 + \|\mathbf{x}_{\mathcal{T}}\|^2}{2}.$$

Thus, the region \mathcal{R}_0 describes the region that is “four times” away from the expected global minimum.

- ii) The region \mathcal{R}_1 is an intersection of two sets of points. The first set implies that $\nabla^2 \mathbb{E}[f(\mathbf{z})]_{\mathcal{T}}$ is not a positive definite matrix and has at least a negative eigenvalue. Thus, \mathcal{R}_1 represents the region in which the function $\mathbb{E}[f(\mathbf{z})]$ has at least one negative curvature.
- iii) The region \mathcal{R}_2 is also an intersection of two sets of points. From the first set, one can easily see that the Wirtinger gradient $\nabla \mathbb{E}[f(\mathbf{z})]_{\mathcal{T}}$ in \mathcal{R}_2 is nonzero.
- iv) Similarly, the region \mathcal{R}_3 characterizes a region in which the Wirtinger gradient $\nabla \mathbb{E}[f(\mathbf{z})]_{\mathcal{T}}$ is nonzero.
- v) Obviously, the region \mathcal{R}_4 describes a region that is close to the expected global minimum $\lambda_{\mathcal{T}} \mathbf{x}_{\mathcal{T}}$ of the function $\mathbb{E}[f(\mathbf{z})]$.

Also, for intuitive understanding, Fig. 1 visualizes the division of regions \mathcal{R}_0 – \mathcal{R}_4 in \mathbb{R}^2 , which is plotted by means of Monte Carlo simulation.

Then, we proceed to characterize the geometric property of the function $f(\mathbf{z})$ in the above five regions, respectively. Our result is mathematically described in the following proposition.

²In describing these regions, we use $\nabla \mathbb{E}[f(\mathbf{z})]_{\mathcal{T}}$ and $\nabla^2 \mathbb{E}[f(\mathbf{z})]_{\mathcal{T}}$, instead of $\nabla f(\mathbf{z})_{\mathcal{T}}$ and $\nabla^2 f(\mathbf{z})_{\mathcal{T}}$, because they can be arbitrarily close to each other (see Lemma 2), but the former is more convenient to compute and apply. Indeed, $\nabla \mathbb{E}[f(\mathbf{z})]_{\mathcal{T}}$ and $\nabla^2 \mathbb{E}[f(\mathbf{z})]_{\mathcal{T}}$ can be given explicitly in closed-form; see (40) and (41).

Proposition 2: When $\mathcal{T} \cap \text{supp}(\mathbf{x}) \neq \emptyset$, there exist constants $C, c > 0$, which depend on the constants $\delta_1, \delta_2, \delta_3$, such that

$$\begin{cases} \|\nabla f(\mathbf{z})_{\mathcal{T}}\| > 0, & \mathbf{z} \in \mathcal{R}_0 \cup \mathcal{R}_2 \cup \mathcal{R}_3, \\ \begin{bmatrix} \mathbf{u}e^{j\phi(\mathbf{z})} \\ \bar{\mathbf{u}}e^{-j\phi(\mathbf{z})} \end{bmatrix}^* \nabla^2 f(\mathbf{z})_{\mathcal{T}} \begin{bmatrix} \mathbf{u}e^{j\phi(\mathbf{z})} \\ \bar{\mathbf{u}}e^{-j\phi(\mathbf{z})} \end{bmatrix} < 0, & \mathbf{z} \in \mathcal{R}_1 \end{cases} \quad (60)$$

holds with probability at least $1 - cm^{-1}$ provided that $m \geq Ck \log k$. Moreover, for any positive constants $\delta_1 < \|\mathbf{x}\|^2 (\|\mathbf{x}\|^2 + \|\mathbf{x}_{\mathcal{T}}\|^2)$ and δ_4 , there exist constants $\delta_2, \delta_3 > 0$ such that

$$\mathbb{C}^{\mathcal{T}} = \bigcup_{j=0}^4 \mathcal{R}_j. \quad (61)$$

This proposition indicates a benign geometric property of function $f(\mathbf{z})$ throughout the subspace $\mathbb{C}^{\mathcal{T}}$ when $\mathcal{T} \cap \text{supp}(\mathbf{x}) \neq \emptyset$. In particular, it allows to locate the exact region of the solution to the subproblem (19).

- i) For any point $\mathbf{z} \in \mathcal{R}_0 \cup \mathcal{R}_2 \cup \mathcal{R}_3$, the gradient $\nabla f(\mathbf{z})_{\mathcal{T}}$ is always nonzero. Thus, the solution to (19) cannot be in this region.
- ii) For any critical point $\mathbf{z} \in \mathcal{R}_1$, if exists, the function $f(\mathbf{z})$ has at least one negative curvature in the $\mathbf{u}e^{j\phi(\mathbf{z})}$ direction. Algorithms such as PGD [29] possess the ability to successfully escape from this point. Thus, the solution to (19) cannot be in \mathcal{R}_1 as well.
- iii) Since the union $\bigcup_{j=0}^4 \mathcal{R}_j$ of five regions covers the entire subspace $\mathbb{C}^{\mathcal{T}}$, and also noting that the solution to (19) is not in $\bigcup_{j=0}^3 \mathcal{R}_j$, it must be in \mathcal{R}_4 . It could be the local minima, local maxima, or saddle points in this region.
- iv) Notice that the local minima of $f(\mathbf{z})$ always exist since $f(\mathbf{z}) \geq 0$. Thus, they must be in \mathcal{R}_4 . By the definition of \mathcal{R}_4 , those local minima are clustered around the expected global minimum $\lambda_{\mathcal{T}} \mathbf{x}_{\mathcal{T}}$ within a distance δ_4 , which can be arbitrarily small. This, therefore, confirms our speculation.
- v) Of course, there might also be saddle points or local maxima of $f(\mathbf{z})$ in \mathcal{R}_4 . It is not clear whether the saddle points have negative curvatures. In this case, the algorithm could get stuck at those points. Nevertheless, this mishap does not affect our subsequent analysis at all. Indeed, as will be seen later, the proof of Theorem 3 only requires to bound the distance between the zero points of $\nabla f(\mathbf{z})_{\mathcal{T}}$ in \mathcal{R}_4 and the expected global minimum. It does not matter which type of zero points they are.

Finally, we consider the case where $\mathcal{T} \supseteq \text{supp}(\mathbf{x})$. In this case, we can obtain a stronger result that all zero points of $\nabla f(\mathbf{z})$ in \mathcal{R}_4 are exactly \mathbf{x} up to a global phase. This leads to the following proposition, which is easy to interpret.

Proposition 3: When $\mathcal{T} \supseteq \text{supp}(\mathbf{x})$, there exist constants $C, c > 0$ such that with probability at least $1 - cm^{-1}$, the solution to the subproblem (19) is exactly \mathbf{x} up to a global phase when $m \geq Ck \log k$.

In summary, we have explored the geometric property for the subproblem (19) of sparse phase retrieval. Our result extends those of [1], [40] from the global case where $\mathbf{z} \in \mathbb{C}^n$ to

$$\mathcal{R}_0 \doteq \{\mathbf{z} \in \mathbb{C}^{\mathcal{T}}: \|\mathbf{z}\|^2 > 2(\|\mathbf{x}\|^2 + \|\mathbf{x}_{\mathcal{T}}\|^2)\}, \quad (55)$$

$$\mathcal{R}_1 \doteq \left\{ \mathbf{z} \in \mathbb{C}^{\mathcal{T}}: \begin{bmatrix} \mathbf{u}e^{j\phi(\mathbf{z})} \\ \bar{\mathbf{u}}e^{-j\phi(\mathbf{z})} \end{bmatrix}^* \nabla^2 \mathbb{E}[f(\mathbf{z})]_{\mathcal{T}} \begin{bmatrix} \mathbf{u}e^{j\phi(\mathbf{z})} \\ \bar{\mathbf{u}}e^{-j\phi(\mathbf{z})} \end{bmatrix} < -\delta_1 \right\} \cap (\mathbb{C}^{\mathcal{T}} \setminus \mathcal{R}_0), \quad (56)$$

$$\mathcal{R}_2 \doteq \left\{ \mathbf{z} \in \mathbb{C}^{\mathcal{T}}: \begin{bmatrix} \mathbf{z} \\ \bar{\mathbf{z}} \end{bmatrix}^* \nabla \mathbb{E}[f(\mathbf{z})]_{\mathcal{T}} < -\delta_2 \right\} \cap (\mathbb{C}^{\mathcal{T}} \setminus \mathcal{R}_0), \quad (57)$$

$$\mathcal{R}_3 \doteq \left\{ \mathbf{z} \in \mathbb{C}^{\mathcal{T}}: \begin{bmatrix} \mathbf{z} - \mathbf{u}e^{j\phi(\mathbf{z})} \\ \bar{\mathbf{z}} - \bar{\mathbf{u}}e^{-j\phi(\mathbf{z})} \end{bmatrix}^* \nabla \mathbb{E}[f(\mathbf{z})]_{\mathcal{T}} > \delta_3, \|\mathbf{z}\|^2 \geq \frac{1}{2}\|\mathbf{x}\|^2 \right\} \cap (\mathbb{C}^{\mathcal{T}} \setminus \mathcal{R}_0), \quad (58)$$

$$\mathcal{R}_4 \doteq \{\mathbf{z} \in \mathbb{C}^{\mathcal{T}}: \text{dist}(\mathbf{z}, \mathbf{u}) < \delta_4\} \cap (\mathbb{C}^{\mathcal{T}} \setminus \mathcal{R}_0), \quad (59)$$

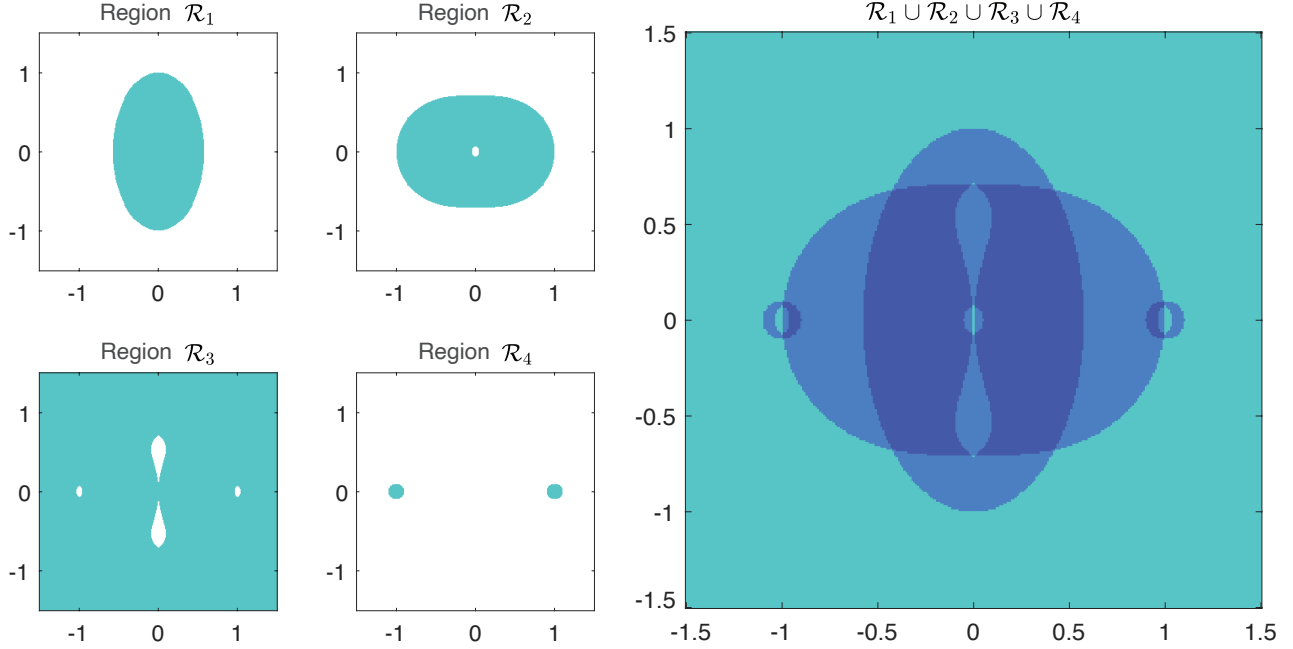


Fig. 1: An illustration of the region division in \mathbb{R}^2 . Here, we suppose that all quantities are real numbers, $\mathcal{T} = \{1, 2\}$, the target solution is $\mathbf{x} = [1, 0]^\top$, and the illustration area is $\{\mathbf{z} \in \mathbb{R}^2 \mid -1.5 \leq z_1 \leq 1.5, -1.5 \leq z_2 \leq 1.5\}$. Regions \mathcal{R}_1 – \mathcal{R}_4 are displayed on the left, marked in blue, while the composition of these four regions is on the right. The overlapped areas are highlighted in darker blue. We omit the illustration of \mathcal{R}_0 since this region is trivial. Clearly the union $\mathcal{R}_1 \cup \mathcal{R}_2 \cup \mathcal{R}_3 \cup \mathcal{R}_4$ can spread over the entire illustration area. One may notice that \mathcal{R}_1 , \mathcal{R}_3 and \mathcal{R}_4 already suffice to cover the illustration area. In other words, \mathcal{R}_0 and \mathcal{R}_2 may be redundant. Nevertheless, the construction of \mathcal{R}_0 and \mathcal{R}_2 brings in much convenience to our analysis, as will be seen in the proof of Proposition 2.

the subspace case where $\mathbf{z} \in \mathbb{C}^{\mathcal{T}}$. In the global case, the global minimum is obviously \mathbf{x} up to a global phase. Whereas in the subspace case, there is no closed-form expression for the local/global minima, which brings difficulties to our analysis. To circumvent the difficulties, we have constructed the region \mathcal{R}_4 to avoid the direct computation of the local/global minima of $f(\mathbf{z})$, while connecting them to the expected global minimum (i.e., $\lambda_{\mathcal{T}} \mathbf{x}_{\mathcal{T}}$) using the concentration inequalities established in Lemma 2. In essence, this allows us to characterize the geometric property of (19) theoretically for the subspace case with finite samples.

We now have all ingredients to prove Theorem 3.

Proof. Without loss of generality, suppose that $S^0 \cap \text{supp}(\mathbf{x}) \neq \emptyset$. This means that at least one support index is chosen in the initialization step.

- Consider the pruning operation in the first iteration of SPR (i.e., $S^1 \leftarrow \mathcal{C}(\mathbf{x}^1, k)$). From Proposition 2, for any $\epsilon_1 > 0$, there exists constants $c_1, C_1 > 0$ such that

$$\text{dist}(\mathbf{x}^1, \lambda_{\hat{S}^1} \mathbf{x}_{\hat{S}^1}) < \epsilon_1 \quad (62)$$

holds with probability at least $1 - c_1 m^{-1}$ when $m \geq C_1 k \log k$. If we rewrite (62) as

$$\|\mathbf{x}^1 - \lambda_{\hat{S}^1} \mathbf{x}_{\hat{S}^1}\| < \epsilon_1 \quad (63)$$

for some complex number $\lambda_{\hat{S}^1}$, then by properly choosing

$$\epsilon_1 < \frac{1}{2} |\lambda_{\hat{S}^1}| \min_{i \in \text{supp}(\mathbf{x})} |x_i|, \quad (64)$$

the largest k elements (in magnitude) of \mathbf{x}^1 should be identical to those of $\lambda_{\hat{S}^1} \mathbf{x}_{\hat{S}^1}$.

Note that $|\text{supp}(\lambda_{\hat{S}^1} \mathbf{x}_{\hat{S}^1})| = |\hat{S}^1 \cap \text{supp}(\mathbf{x})| \leq k$ and that the pruning operation narrows down the candidates in \hat{S}^1 to k corresponding to the largest k entries (in magnitude) of \mathbf{x}^1 . Therefore, with probability at least $1 - c_1 m^{-1}$, we have

$$S^1 \supseteq \hat{S}^1 \cap \text{supp}(\mathbf{x}). \quad (65)$$

- Consider the matching operation in the second iteration (i.e., $\hat{S}^2 \leftarrow S^1 \cup \mathcal{C}(\nabla_1 f(\mathbf{x}^1), k)$). Instead of finding out the support of $\nabla_1 f(\mathbf{x}^1)$ directly, we first compute $\nabla_1 \mathbb{E}[f(\lambda_{\hat{S}^1} \mathbf{x}_{\hat{S}^1})]$ as:

$$\nabla_1 \mathbb{E}[f(\lambda_{\hat{S}^1} \mathbf{x}_{\hat{S}^1})] = \lambda_{\hat{S}^1} \|\mathbf{x}_{\hat{S}^1}\|^2 (\mathbf{x}_{\hat{S}^1} - \mathbf{x}). \quad (66)$$

Hence, $\nabla_1 \mathbb{E}[f(\lambda_{\hat{S}^1} \mathbf{x}_{\hat{S}^1})]$ is supported on $\text{supp}(\mathbf{x}) \setminus \hat{S}^1$. Then, we shall provide a condition guaranteeing $\nabla_1 f(\mathbf{x}^1)$ and $\nabla_1 \mathbb{E}[f(\lambda_{\hat{S}^1} \mathbf{x}_{\hat{S}^1})]$ to have the identical support.

Using the triangle inequality, we can bound the distance between $\nabla_1 f(\mathbf{x}^1)$ and $\nabla_1 \mathbb{E}[f(\lambda_{\hat{S}^1} \mathbf{x}_{\hat{S}^1})]$ as follows:

$$\begin{aligned} & \|\nabla_1 f(\mathbf{x}^1) - \nabla_1 \mathbb{E}[f(\lambda_{\hat{S}^1} \mathbf{x}_{\hat{S}^1})]\| \\ & \leq \|\nabla_1 f(\mathbf{x}^1) - \nabla_1 \mathbb{E}[f(\mathbf{x}^1)]\| \\ & \quad + \|\nabla_1 \mathbb{E}[f(\mathbf{x}^1)] - \nabla_1 \mathbb{E}[f(\lambda_{\hat{S}^1} \mathbf{x}_{\hat{S}^1})]\|. \end{aligned} \quad (67)$$

We shall bound the two terms on the right-hand side of (67), respectively.

From Lemma 2, for any $\epsilon_2 > 0$, there exist constants $c_2, C_2 > 0$ such that with probability at least $1 - c_2 m^{-1}$,

$$\|\nabla_1 f(\mathbf{x}^1) - \nabla_1 \mathbb{E}[f(\mathbf{x}^1)]\| < \epsilon_2 \quad (68)$$

when $m \geq C_2 k \log k$. From Proposition 2, there exist constants $c_3, C_3 > 0$ such that with probability at least $1 - c_3 m^{-1}$,

$$\|\mathbf{x}^1 - \lambda_{\hat{S}^1} \mathbf{x}_{\hat{S}^1}\| < \delta(\epsilon_3) \quad (69)$$

when $m \geq C_3 k \log k$. Considering the continuity of $\nabla_1 \mathbb{E}[f(\mathbf{z})]$ with respect to \mathbf{z} , it is clear that for any $\epsilon_3 > 0$, there exists $\delta(\epsilon_3) > 0$ such that

$$\|\mathbb{E}[f(\mathbf{x}^1)] - \mathbb{E}[f(\lambda_{\hat{S}^1} \mathbf{x}_{\hat{S}^1})]\| < \epsilon_3 \quad (70)$$

holds under (69).

By taking the values

$$0 < \epsilon_2 = \epsilon_3 < \frac{1}{4} |\lambda_{\hat{S}^1}| \|\mathbf{x}_{\hat{S}^1}\|^2 \min_{i \in \text{supp}(\mathbf{x})} |x_i|, \quad (71)$$

in (68) and (70), we have that with probability at least $1 - (c_2 + c_3)m^{-1}$, the left-hand side of (67) is upper bounded by

$$\begin{aligned} & \|\nabla_1 f(\mathbf{x}^1) - \nabla_1 \mathbb{E}[f(\lambda_{\hat{S}^1} \mathbf{x}_{\hat{S}^1})]\| \\ & \leq \frac{1}{2} |\lambda_{\hat{S}^1}| \|\mathbf{x}_{\hat{S}^1}\|^2 \min_{i \in \text{supp}(\mathbf{x})} |x_i|. \end{aligned} \quad (72)$$

This, together with (66), implies that the k largest elements (in magnitude) of $\nabla_1 f(\mathbf{x}^1)$ coincide with those of $\nabla_1 \mathbb{E}[f(\lambda_{\hat{S}^1} \mathbf{x}_{\hat{S}^1})]$. As a result,

$$\begin{aligned} \mathcal{C}(\nabla_1 f(\mathbf{x}^1), k) & \supseteq \text{supp}(\nabla_1 \mathbb{E}[f(\lambda_{\hat{S}^1} \mathbf{x}_{\hat{S}^1})]) \\ & \stackrel{(66)}{=} \text{supp}(\mathbf{x}) \setminus \hat{S}^1. \end{aligned} \quad (73)$$

Finally, using (65) and (73), we obtain the result of the matching operation as

$$\begin{aligned} \hat{S}^2 & = S^1 \cup \mathcal{C}(\nabla_1 f(\mathbf{x}^1), k) \\ & \stackrel{(65), (73)}{\supseteq} (\hat{S}^1 \cap \text{supp}(\mathbf{x})) \cup (\text{supp}(\mathbf{x}) \setminus \hat{S}^1) \\ & = \text{supp}(\mathbf{x}). \end{aligned} \quad (74)$$

In summary, when $m \geq \max\{C_1, C_2, C_3\} k \log k$, $\text{supp}(\mathbf{x}) \subset \hat{S}^2$ holds with probability at least $1 - (c_1 + c_2 + c_3)m^{-1}$. In other words, we can get an estimated support \hat{S}^2 of size $2k$ that contains all the support indices of \mathbf{x} . By applying Proposition 3), we can conclude that SPR recovers the signal \mathbf{x} exactly (up to a global phase). This completes the proof. \square

IV. EXPERIMENTS

In this section, numerical experiments are carried out to test the performance of SPR for phase retrieval. Our experiments are performed in the MATLAB 2019a environment on a server with a Intel(R) Xeon(R) Silver 4116 CPU and 4 GeForce RTX 2080 Ti GPUs.

A. Geometric Property

We empirically verify the geometric property in Proposition 2. Specifically, we construct a random matrix $\mathbf{A} \in \mathbb{C}^{10,000 \times 20,000}$ with entries drawn *i.i.d.* from the standard complex Gaussian distribution. Also, we generate a vector $\mathbf{x} \in \mathbb{C}^{10,000}$ whose first 10 entries are 1 and the rest are 0. Then, we use the BB algorithm [30] to find out the solution $\hat{\mathbf{x}}$ to (19) over the estimated support $\mathcal{T} = \{1, \dots, 5, 11, \dots, 25\}$. In this case, $\mathcal{T} \cup \text{supp}(\mathbf{x}) = \{1, \dots, 5\} \neq \emptyset$.

In Fig. 2, blue points represent the expected global optimum (i.e., $\lambda_{\mathcal{T}} \mathbf{x}_{\mathcal{T}}$), while red points are the numerical solution to (19). Since the original values of the solution are complex numbers, we plot their modulus for illustration. One can observe that the numerical solution is well clustered around the expected global optimum, which matches the proposed geometric property.

B. Recovery of 1D signals

The original signal $\mathbf{x} \in \mathbb{C}^{1,000}$ has sparsity $k = 10$. Each entry of A and the nonzero elements of \mathbf{x} are drawn *i.i.d.* from the standard complex Gaussian distribution. The number m of measurements varies from 100 to 2,000 with step 100. For comparative purpose, SPARTA [20], SWF [21], WF [15], TWF [17], TAF [41], and RWF [16] are included. The codes of SPARTA and SWF are from <https://gangwg.github.io/SPARTA/index.html> and <https://github.com/Ziyang1992/Sparse-Wirtinger-flow>, respectively. The codes of other testing algorithms are from PhasePack [42]. To measure the error between the recovered signal $\hat{\mathbf{x}}$ and the original signal \mathbf{x} , we use the normalized mean squared error (NMSE), which is defined as

$$\text{NMSE} \doteq \frac{\text{dist}(\mathbf{x}, \hat{\mathbf{x}})}{\|\mathbf{x}\|}. \quad (75)$$

The signal recovery is considered successful if the NMSE between the original signal \mathbf{x} and the recovered signal $\hat{\mathbf{x}}$

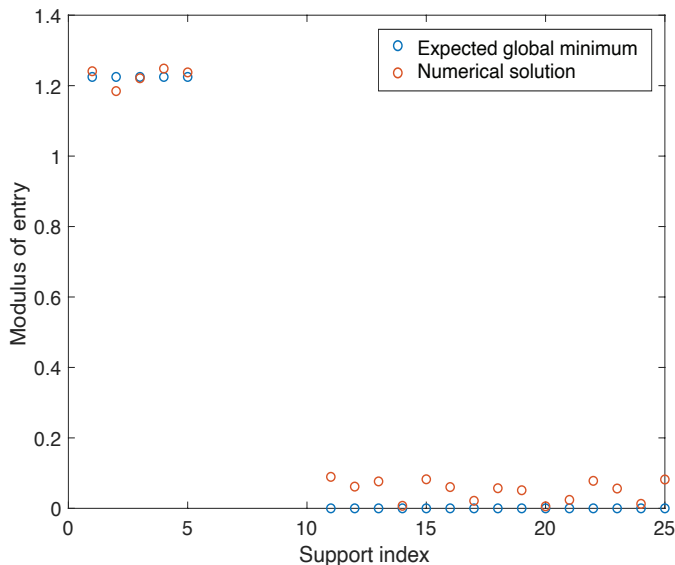


Fig. 2: The numerical solution is clustered around the expected global minimum.

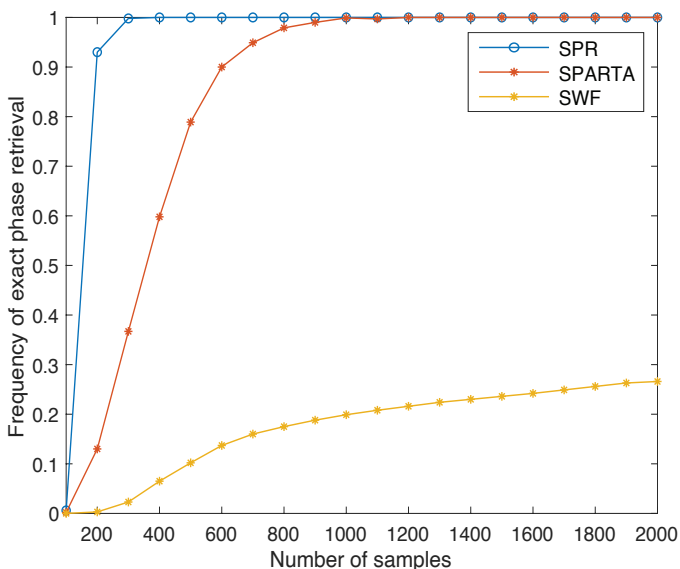


Fig. 3: Frequency of exact phase retrieval as a function of the number of samples.

is smaller than 10^{-6} . We use the frequency of exact phase retrieval as a performance metric to evaluate the performance of different algorithms.

Figure 3 shows the performance of different algorithms. Overall, we observe that SPR performs uniformly better than other algorithms for the whole testing region of m . In particular, it achieves 100% exact phase retrieval ratio when m is only 300, while SPARTA requires the number of samples to be at least 1,000, and SWF recovers the signal with the success ratio lower than 30% when $m \leq 2,000$. For the remaining algorithms (i.e., WF, TWF, TAF and RWF) that do not exploit the sparse prior, the frequency of exact phase retrieval is around zero when $m \leq 2,000$. This demonstrates that exploiting the signal sparsity is beneficial for phase

retrieval, especially when the sampling number is small.

C. Recovery of 2D image

We consider the recovery of signals from Fourier samples. In this case, the matching step of SPR allows fast implementation. Specifically, the Wirtinger derivative can be computed efficiently via the fast Fourier transform (FFT):

$$\begin{aligned} \nabla_1 f(\mathbf{z}) &= \frac{1}{m} \sum_{i=1}^m (|\mathbf{a}_i^* \mathbf{z}|^2 - y_i^2) (\mathbf{a}_i \mathbf{a}_i^*) \mathbf{z} \\ &= \frac{2}{m} \text{ifft}[\mathbf{u}], \end{aligned} \quad (76)$$

where

$$u_i = ((\text{fft}[\mathbf{z}])_i^2 - y_i^2) (\text{fft}[\mathbf{z}])_i^2, \quad i = 1, \dots, n,$$

and fft and ifft denote the FFT and inverse FFT, respectively. When the signal \mathbf{x} is an $n \times n$ image, fft is replaced with fft2 , i.e., the 2D FFT. Then, the sampling model is given by

$$\mathbf{Y} = \mathbf{F} \mathbf{X} \mathbf{F}^\top, \quad (77)$$

where \mathbf{F} is Fourier transformation matrix. fft2 (i.e., $\mathbf{Y} = \text{fft2}(\mathbf{X})$) can save some matrix operations to speed up the computation. The task of phase retrieval is to recover the original image \mathbf{x} from the amplitudes of elements in \mathbf{Y} .

Figure 4 shows the recovery result for a 2D Tai-Chi image of size 300×300 , whose sparsity is approximately 430. We conduct the 2D Fourier transform on this image and solve the phase retrieval problem. Since there exist various ill-posed properties in Fourier cases, such as global phase shift, conjugate inversion, spatial shift, and even multiple solutions, we do not give stringent criteria for successful recovery. Instead, we directly compare the recovered image with the ground truth. To clearly show the recovery result, we center the Tai-Chi symbol and crop it into a smaller size of 81×81 . One can observe that the recovery quality of SPR is much better than that of HIO, which demonstrates the superiority of the proposed SPR algorithm.

V. CONCLUSION

In recent years, phase retrieval has received much attention in many fields such as optical imaging. In this paper, we have proposed a greedy algorithm called SPR for phase retrieval. Our algorithm is able to reconstruct any sparse signal when the number of magnitude-only samples is nearly linear in the sparsity level of the signal. The result offers a significant improvement over previous works, and also close the gap to the information-theoretic bound for the sparse phase retrieval problem. Numerical experiments have demonstrated that SPR has competitive recovery quality compared to the state-of-the-art techniques for phase retrieval, especially when the number of samples is small. On account of the fast convergence and ease of implementation (e.g., no need to know the support of input signal in advance), the proposed SPR approach can serve as an attractive alternative to the classic HIO [9] method for phase retrieval.

We would like to point out some directions worth of future investigation. First of all, while in this paper we are primarily

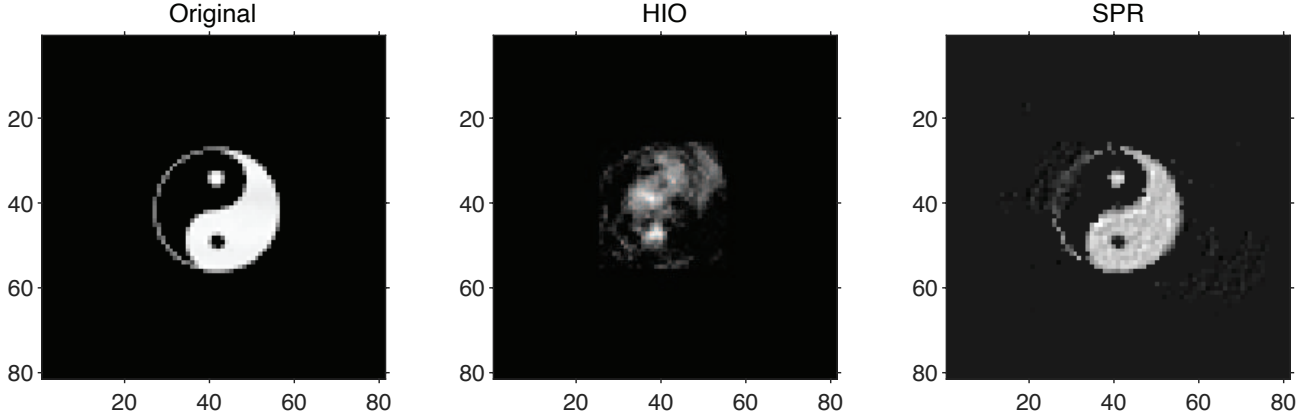


Fig. 4: Comparison of reconstruction results for the Tai-Chi image using HIO and SPR.

interested in analyzing SPR with complex Gaussian samples, the SPR algorithm nevertheless shows promising reconstruction result empirically for Fourier samples. Thus we believe that our theoretical results may hold for the Fourier case as well. In essence, this would require that Fourier samples satisfy some concentration inequalities analogous to those in Lemma 2. The second direction concerns the performance guarantee of SPR in the presence of noise. A favorable geometric property and some techniques in [43], [44] may offer a route to a theoretical guarantee for this scenario and help to uncover the whole story of SPR. At present, this remains a topic of ongoing work.

APPENDIX A PROOF OF LEMMA 2

We first present a useful lemma on the concentration of random Gaussian matrices.

Lemma 3 (Lemma 6.3 in [1]): Suppose that the entries of matrix $\mathbf{A} \in \mathbb{C}^{m \times n}$ are *i.i.d.* copies of the standard complex Gaussian distribution. Then, for any constant $\delta > 0$ and any vector $\mathbf{v} \in \mathbb{C}^n$ supported on \mathcal{T} where $|\mathcal{T}| = k$, the following inequalities hold with probability exceeding $1 - c_a \delta^{-2} m^{-1} - c_b \exp(-c_c \delta^2 m / \log m)$ when $m \geq Ck \log k$,

$$\left\| \left(\frac{1}{m} \sum_{k=1}^m |\mathbf{a}_k^* \mathbf{v}|^2 \mathbf{a}_k \mathbf{a}_k^* - (\mathbf{v} \mathbf{v}^* + \|\mathbf{v}\|^2 \mathbf{I}) \right)_{\mathcal{T}} \right\| \leq \delta \|\mathbf{v}\|^2, \quad (78)$$

$$\left\| \left(\frac{1}{m} \sum_{k=1}^m (\mathbf{a}_k^* \mathbf{v})^2 \mathbf{a}_k \mathbf{a}_k^T - 2\mathbf{v} \mathbf{v}^T \right)_{\mathcal{T}} \right\| \leq \delta \|\mathbf{v}\|^2. \quad (79)$$

Now we are ready to prove our lemma.

Proof. Define

$$\mathbf{A}_{\mathbf{z}} = \frac{1}{m} \sum_{k=1}^m |\mathbf{a}_k^* \mathbf{z}|^2 \mathbf{a}_k \mathbf{a}_k^* - \mathbf{z} \mathbf{z}^* - \|\mathbf{z}\|^2 \mathbf{I}, \quad (80)$$

$$\mathbf{B}_{\mathbf{z}} = \frac{1}{m} \sum_{k=1}^m (\mathbf{a}_k^* \mathbf{z})^2 \mathbf{a}_k \mathbf{a}_k^T - 2\mathbf{z} \mathbf{z}^T. \quad (81)$$

Then, the difference between $\nabla^2 f(\mathbf{z})_{\mathcal{T}}$ and $\nabla^2 \mathbb{E}[f(\mathbf{z})]_{\mathcal{T}}$ can be given by

$$\begin{aligned} & \nabla^2 f(\mathbf{z})_{\mathcal{T}} - \nabla^2 \mathbb{E}[f(\mathbf{z})]_{\mathcal{T}} \\ &= \begin{bmatrix} (2\mathbf{A}_{\mathbf{z}} - \mathbf{A}_{\mathbf{x}})_{\mathcal{T}} & (\mathbf{B}_{\mathbf{z}})_{\mathcal{T}} \\ (\bar{\mathbf{B}}_{\mathbf{z}})_{\mathcal{T}} & (2\bar{\mathbf{A}}_{\mathbf{z}} - \bar{\mathbf{A}}_{\mathbf{x}})_{\mathcal{T}} \end{bmatrix}. \end{aligned} \quad (82)$$

Denote $\tilde{\mathcal{T}} \doteq \mathcal{T} \cup \text{supp}(\mathbf{x})$. By applying Lemma 3 with $\mathbf{v} = \mathbf{z}$ and $\mathbf{x} = \mathbf{x}$, respectively, we have that for any constant $\delta > 0$, the following inequalities hold with probability at least $1 - cm^{-1}$,

$$\left\| \begin{bmatrix} (\mathbf{A}_{\mathbf{z}})_{\mathcal{T}} & \mathbf{0} \\ \mathbf{0} & (\bar{\mathbf{A}}_{\mathbf{z}})_{\mathcal{T}} \end{bmatrix} \right\| = \|(\mathbf{A}_{\mathbf{z}})_{\mathcal{T}}\| \leq \delta \|\mathbf{z}\|^2, \quad (83)$$

$$\left\| \begin{bmatrix} \mathbf{0} & (\mathbf{B}_{\mathbf{z}})_{\mathcal{T}} \\ (\mathbf{B}_{\mathbf{z}})_{\mathcal{T}} & \mathbf{0} \end{bmatrix} \right\| = \|(\mathbf{B}_{\mathbf{z}})_{\mathcal{T}}\| \leq \delta \|\mathbf{z}\|^2, \quad (84)$$

$$\left\| \begin{bmatrix} (\mathbf{A}_{\mathbf{x}})_{\mathcal{T}} & \mathbf{0} \\ \mathbf{0} & (\bar{\mathbf{A}}_{\mathbf{x}})_{\mathcal{T}} \end{bmatrix} \right\| = \|(\mathbf{A}_{\mathbf{x}})_{\mathcal{T}}\| \stackrel{(a)}{\leq} \|(\mathbf{A}_{\mathbf{x}})_{\tilde{\mathcal{T}}}\| \leq \delta \|\mathbf{x}\|^2, \quad (85)$$

when $m \geq Ck \log k$, where (a) is due to the Cauchy's interlace theorem. Therefore,

$$\|\nabla^2 f(\mathbf{z})_{\mathcal{T}} - \nabla^2 \mathbb{E}[f(\mathbf{z})]_{\mathcal{T}}\| \leq \delta (3\|\mathbf{z}\|^2 + \|\mathbf{x}\|^2). \quad (86)$$

Next, we shall bound the difference between $\nabla f(\mathbf{z})_{\mathcal{T}}$ and $\mathbb{E}[\nabla f(\mathbf{z})]_{\mathcal{T}}$ by means of Lemma 3.

Under the same condition, we have

$$\begin{aligned}
& \|\nabla f(\mathbf{z})_{\mathcal{T}} - \mathbb{E}[\nabla f(\mathbf{z})]_{\mathcal{T}}\| \\
&= \sqrt{2} \left\| \left(\frac{1}{m} \sum_{k=1}^m \left((|\mathbf{a}_k^* \mathbf{z}|^2 - y_k^2) \mathbf{a}_k \mathbf{a}_k^* \right)_{\mathcal{T}} \right. \right. \\
&\quad \left. \left. - (2\|\mathbf{z}\|^2 - \|\mathbf{x}\|^2) \mathbf{I}_{\mathcal{T}} + \mathbf{x}_{\mathcal{T}} \mathbf{x}_{\mathcal{T}}^* \right) \mathbf{z} \right\| \\
&\leq \sqrt{2} \|\mathbf{z}\| \left\| \left(\frac{1}{m} \sum_{k=1}^m |\mathbf{a}_k^* \mathbf{z}|^2 \mathbf{a}_k \mathbf{a}_k^* - (\|\mathbf{z}\|^2 \mathbf{I} + \mathbf{z} \mathbf{z}^*) \right)_{\mathcal{T}} \right\| \\
&\quad + \left\| \left(\frac{1}{m} \sum_{k=1}^m |\mathbf{a}_k^* \mathbf{x}|^2 \mathbf{a}_k \mathbf{a}_k^* - (\|\mathbf{x}\|^2 \mathbf{I} + \mathbf{x} \mathbf{x}^*) \right)_{\mathcal{T}} \right\| \\
&\leq \sqrt{2} \|\mathbf{z}\| \left\| \left(\frac{1}{m} \sum_{k=1}^m |\mathbf{a}_k^* \mathbf{z}|^2 \mathbf{a}_k \mathbf{a}_k^* - (\|\mathbf{z}\|^2 \mathbf{I} + \mathbf{z} \mathbf{z}^*) \right)_{\mathcal{T}} \right\| \\
&\quad + \left\| \left(\frac{1}{m} \sum_{k=1}^m |\mathbf{a}_k^* \mathbf{x}|^2 \mathbf{a}_k \mathbf{a}_k^* - (\|\mathbf{x}\|^2 \mathbf{I} + \mathbf{x} \mathbf{x}^*) \right)_{\mathcal{T}} \right\|, \quad (87)
\end{aligned}$$

where the last inequality is from Cauchy's interlace theorem.

By applying Lemma 3 with $\mathbf{v} = \mathbf{z}$ and $\mathbf{x} = \mathbf{x}$, we can conclude that

$$\|\nabla f(\mathbf{z})_{\mathcal{T}} - \mathbb{E}[\nabla f(\mathbf{z})]_{\mathcal{T}}\| \leq \sqrt{2} \delta \|\mathbf{z}\| (\|\mathbf{x}\|^2 + \|\mathbf{z}\|^2). \quad (88)$$

The proof is thus complete. \square

APPENDIX B PROOFS OF PROPOSITIONS

A. Proof of Proposition 1

Proof. We consider the following cases.

- i) It is trivial that $\mathbf{z} = 0$ is the zero point of $\nabla \mathbb{E}[f(\mathbf{z})]_{\mathcal{T}}$. Also, it is obvious that

$$\nabla^2 \mathbb{E}[f(0)]_{\mathcal{T}} \prec 0. \quad (89)$$

Thus $\mathbf{z} = 0$ is the local maximum of $\mathbb{E}[f(\mathbf{z})]$ in the subspace $\mathbb{C}^{\mathcal{T}}$.

- ii) In the region of $\{\mathbf{z} \in \mathbb{C}^{\mathcal{T}} : 0 < \|\mathbf{z}\|^2 < \frac{1}{2} \|\mathbf{x}\|^2\}$, observe that

$$\begin{bmatrix} \mathbf{z} \\ \bar{\mathbf{z}} \end{bmatrix}^* \nabla \mathbb{E}[f(\mathbf{z})]_{\mathcal{T}} = 2(2\|\mathbf{z}\|^2 - \|\mathbf{x}\|^2) \|\mathbf{z}\|^2 - 2|\mathbf{x}_{\mathcal{T}}^* \mathbf{z}|^2 < 0. \quad (90)$$

Thus, there is no zero point of $\nabla \mathbb{E}[f(\mathbf{z})]_{\mathcal{T}}$ in this region.

- iii) When $\|\mathbf{z}\|^2 = \frac{1}{2} \|\mathbf{x}\|^2$,

$$\nabla \mathbb{E}[f(\mathbf{z})]_{\mathcal{T}} = \begin{bmatrix} -\mathbf{x}_{\mathcal{T}} \mathbf{x}_{\mathcal{T}}^* \mathbf{z} \\ -\bar{\mathbf{x}}_{\mathcal{T}} \mathbf{x}_{\mathcal{T}}^* \bar{\mathbf{z}} \end{bmatrix}. \quad (91)$$

So

$$\begin{aligned}
\nabla \mathbb{E}[f(\mathbf{z})]_{\mathcal{T}} = 0 &\Leftrightarrow \mathbf{z} \in \text{Null}(\mathbf{x}_{\mathcal{T}} \mathbf{x}_{\mathcal{T}}^*) \\
&\Leftrightarrow \mathbf{x}_{\mathcal{T}}^* \mathbf{z} = 0 \\
&\Leftrightarrow \mathbf{x}^* \mathbf{z} = 0. \quad (92)
\end{aligned}$$

Further, any point in \mathcal{S} is the zero point of $\nabla \mathbb{E}[f(\mathbf{z})]_{\mathcal{T}}$. Besides, for any $\mathbf{z} \in \mathcal{S}$, it holds that

$$\begin{aligned}
\begin{bmatrix} \mathbf{x}_{\mathcal{T}} e^{j\phi(\mathbf{z})} \\ \bar{\mathbf{x}}_{\mathcal{T}} e^{-j\phi(\mathbf{z})} \end{bmatrix}^* \nabla^2 \mathbb{E}[f(\mathbf{z})]_{\mathcal{T}} \begin{bmatrix} \mathbf{x}_{\mathcal{T}} e^{j\phi(\mathbf{z})} \\ \bar{\mathbf{x}}_{\mathcal{T}} e^{-j\phi(\mathbf{z})} \end{bmatrix} &= -2\|\mathbf{x}_{\mathcal{T}}\|^4 \\
&< 0, \quad (93)
\end{aligned}$$

and

$$\begin{bmatrix} \mathbf{z} \\ \bar{\mathbf{z}} \end{bmatrix}^* \nabla^2 \mathbb{E}[f(\mathbf{z})]_{\mathcal{T}} \begin{bmatrix} \mathbf{z} \\ \bar{\mathbf{z}} \end{bmatrix} = 8\|\mathbf{z}\|^2 > 0. \quad (94)$$

Hence, any $\mathbf{z} \in \mathcal{S}$ is the saddle point of $\mathbb{E}[f(\mathbf{z})]$ on $\mathbb{C}^{\mathcal{T}}$.

- iv) Consider the region of $\{\mathbf{z} \in \mathbb{C}^{\mathcal{T}} : \|\mathbf{z}\|^2 > \frac{1}{2} \|\mathbf{x}\|^2\}$. From (40), the zero points of $\nabla_1 \mathbb{E}[f(\mathbf{z})]_{\mathcal{T}}$ satisfy

$$(2\|\mathbf{z}\|^2 - \|\mathbf{x}\|^2) \mathbf{z} = \mathbf{x}_{\mathcal{T}} \mathbf{x}_{\mathcal{T}}^* \mathbf{z}, \quad (95)$$

which implies that $2\|\mathbf{z}\|^2 - \|\mathbf{x}\|^2$ is an eigenvalue of the matrix $\mathbf{x}_{\mathcal{T}} \mathbf{x}_{\mathcal{T}}^*$. Since $\mathbf{x}_{\mathcal{T}} \mathbf{x}_{\mathcal{T}}^*$ is a rank-one semidefinite positive Hermite matrix $\mathbf{x}_{\mathcal{T}} \mathbf{x}_{\mathcal{T}}^*$, and also noting that \mathbf{z} satisfies $2\|\mathbf{z}\|^2 - \|\mathbf{x}\|^2 > 0$ in this given region, the nonzero eigenvalue of $\mathbf{x}_{\mathcal{T}} \mathbf{x}_{\mathcal{T}}^*$ must be $2\|\mathbf{z}\|^2 - \|\mathbf{x}\|^2$. We can further deduce that

$$\begin{aligned}
2\|\mathbf{z}\|^2 - \|\mathbf{x}\|^2 &= \lambda_{\max}(\mathbf{x}_{\mathcal{T}} \mathbf{x}_{\mathcal{T}}^*) \\
&= \text{Tr}(\mathbf{x}_{\mathcal{T}} \mathbf{x}_{\mathcal{T}}^*) \\
&= \text{Tr}(\mathbf{x}_{\mathcal{T}}^* \mathbf{x}_{\mathcal{T}}) \\
&= \|\mathbf{x}_{\mathcal{T}}\|^2. \quad (96)
\end{aligned}$$

That is,

$$\|\mathbf{z}\| = \sqrt{\frac{\|\mathbf{x}\|^2 + \|\mathbf{x}_{\mathcal{T}}\|^2}{2}}. \quad (97)$$

Plugging it into (95) yields

$$\|\mathbf{x}_{\mathcal{T}}\|^2 \mathbf{z} = \mathbf{x}_{\mathcal{T}} \mathbf{x}_{\mathcal{T}}^* \mathbf{z}. \quad (98)$$

Thus, the zero points of $\nabla_1 \mathbb{E}[f(\mathbf{z})]_{\mathcal{T}}$ located in the given region satisfy both (97) and (98). It is easily verified that the zero point in this region is uniquely given by

$$\mathbf{z} = \lambda_{\mathcal{T}} \mathbf{x}_{\mathcal{T}}. \quad (99)$$

where $\lambda_{\mathcal{T}} \in \mathbb{C}$ and $|\lambda_{\mathcal{T}}| = \sqrt{\frac{\|\mathbf{x}\|^2 + \|\mathbf{x}_{\mathcal{T}}\|^2}{2\|\mathbf{x}_{\mathcal{T}}\|^2}}$.

Our remaining task is to show $\mathbf{z} = \lambda_{\mathcal{T}} \mathbf{x}_{\mathcal{T}}$ is not only a unique zero point of $\mathbb{E}[f(\mathbf{z})]$ in the region of $\{\mathbf{z} \in \mathbb{C}^{\mathcal{T}} : \|\mathbf{z}\|^2 > \frac{1}{2} \|\mathbf{x}\|^2\}$, but also is the local minimum of $\mathbb{E}[f(\mathbf{z})]$ for the whole subspace $\mathbf{z} \in \mathbb{C}^{\mathcal{T}}$. To the end, recall from (39) that

$$\begin{aligned}
\mathbb{E}[f(\mathbf{z})] &= \|\mathbf{x}\|^4 + \|\mathbf{z}\|^4 - \|\mathbf{x}\|^2 \|\mathbf{z}\|^2 - |\mathbf{x}^* \mathbf{z}|^2 \\
&= \|\mathbf{z}\|^4 - \left(\|\mathbf{x}\|^2 + \left| \mathbf{x}^* \left(\frac{\mathbf{z}}{\|\mathbf{z}\|} \right) \right|^2 \right) \|\mathbf{z}\|^2 + \|\mathbf{x}\|^4,
\end{aligned}$$

which attains its minimum when $\left| \mathbf{x}^* \left(\frac{\mathbf{z}}{\|\mathbf{z}\|} \right) \right|^2$ is maximized, that is, when

$$\mathbf{z} = \rho \mathbf{x}_{\mathcal{T}} \quad (100)$$

where $\rho \in \mathbb{C}$ and $|\rho| = \frac{\|\mathbf{z}\|}{\|\mathbf{x}_{\mathcal{T}}\|}$. Then, we can rewrite $\mathbb{E}[f(\mathbf{z})]$ as

$$\begin{aligned}
\mathbb{E}[f(\mathbf{z})] &= \|\mathbf{x}\|^4 + |\rho|^4 \|\mathbf{x}_{\mathcal{T}}\|^4 - |\rho|^2 \|\mathbf{x}\|^2 \|\mathbf{x}_{\mathcal{T}}\|^2 - |\rho|^2 \|\mathbf{x}_{\mathcal{T}}\|^4 \\
&= \|\mathbf{x}_{\mathcal{T}}\|^4 |\rho|^4 - (\|\mathbf{x}\|^2 \|\mathbf{x}_{\mathcal{T}}\|^2 + \|\mathbf{x}_{\mathcal{T}}\|^4) |\rho|^2 + \|\mathbf{x}\|^4.
\end{aligned}$$

Clearly this is a second-order polynomial of $|\rho|^2$, which attains the minimum when

$$|\rho| = \sqrt{\frac{\|\mathbf{x}\|^2 + \|\mathbf{x}_{\mathcal{T}}\|^2}{2\|\mathbf{x}_{\mathcal{T}}\|^2}} = |\lambda_{\mathcal{T}}|. \quad (101)$$

Therefore, $\mathbf{z} = \lambda_{\mathcal{T}} \mathbf{x}_{\mathcal{T}}$ is the local minimum of $\mathbb{E}[f(\mathbf{z})]$ for $\mathbf{z} \in \mathbb{C}^{\mathcal{T}}$.

The proposition is established by combining the results of the above four cases. \square

B. Proof of Proposition 2

Proof. Our proof relies on some techniques developed in [1]. We partition the proof into two parts. First, we show that with probability exceeding $1 - cm^{-1}$

$$\begin{cases} \|\nabla f(\mathbf{z})_{\mathcal{T}}\| > 0, & \mathbf{z} \in \mathcal{R}_0 \cup \mathcal{R}_2 \cup \mathcal{R}_3, \\ \begin{bmatrix} \mathbf{u}e^{j\phi(\mathbf{z})} \\ \bar{\mathbf{u}}e^{-j\phi(\mathbf{z})} \end{bmatrix}^* \nabla^2 f(\mathbf{z})_{\mathcal{T}} \begin{bmatrix} \mathbf{u}e^{j\phi(\mathbf{z})} \\ \bar{\mathbf{u}}e^{-j\phi(\mathbf{z})} \end{bmatrix} < 0, & \mathbf{z} \in \mathcal{R}_1, \end{cases} \quad (102)$$

when $m \geq Ck \log k$. In the second part, we show that $\mathbb{C}^{\mathcal{T}} = \cup_{j=0}^4 \mathcal{R}_j$ and the solution to (19) is located in \mathcal{R}_4 .

Part 1: To show the result of the first part, we consider the following four cases.

i) For any $\mathbf{z} \in \mathcal{R}_0 = \{\mathbf{z} \in \mathbb{C}^{\mathcal{T}} : \|\mathbf{z}\|^2 > 2(\|\mathbf{x}\|^2 + \|\mathbf{x}_{\mathcal{T}}\|^2)\}$, we have

$$\begin{aligned} & \|\nabla \mathbb{E}[f(\mathbf{z})]_{\mathcal{T}}\|^2 \\ & \stackrel{(40)}{=} \|((2\|\mathbf{z}\|^2 - \|\mathbf{x}\|^2)\mathbf{I} - \mathbf{x}_{\mathcal{T}}\mathbf{x}_{\mathcal{T}}^*)\mathbf{z}\|^2 \\ & = 2 \left((2\|\mathbf{z}\|^2 - \|\mathbf{x}\|^2)^2 \|\mathbf{z}\|^2 \right. \\ & \quad \left. - (4\|\mathbf{z}\|^2 - 2\|\mathbf{x}\|^2 - \|\mathbf{x}_{\mathcal{T}}\|^2) |\mathbf{x}_{\mathcal{T}}^* \mathbf{z}|^2 \right) \\ & \geq 2 \left((2\|\mathbf{z}\|^2 - \|\mathbf{x}\|^2)^2 \|\mathbf{z}\|^2 \right. \\ & \quad \left. - (4\|\mathbf{z}\|^2 - 2\|\mathbf{x}\|^2 - \|\mathbf{x}_{\mathcal{T}}\|^2) \|\mathbf{x}_{\mathcal{T}}\|^2 \|\mathbf{z}\|^2 \right) \\ & = 2\|\mathbf{z}\|^2 \left(4\|\mathbf{z}\|^2 (\|\mathbf{z}\|^2 - \|\mathbf{x}\|^2 - \|\mathbf{x}_{\mathcal{T}}\|^2) \right. \\ & \quad \left. + (\|\mathbf{x}\|^2 + \|\mathbf{x}_{\mathcal{T}}\|^2)^2 \right) \\ & > 4\|\mathbf{z}\|^6. \end{aligned} \quad (103)$$

Applying Lemma 2 with $\delta = \frac{2}{3}\sqrt{2}$, we have that there exist positive constants c, C such that when $m > Ck \log k$, with probability exceeding $1 - cm^{-1}$,

$$\begin{aligned} \|\nabla f(\mathbf{z})_{\mathcal{T}} - \nabla \mathbb{E}[f(\mathbf{z})]_{\mathcal{T}}\| & \leq \sqrt{2}\delta \|\mathbf{z}\| (\|\mathbf{x}\|^2 + \|\mathbf{z}\|^2) \\ & = \frac{4}{3} \|\mathbf{z}\| (\|\mathbf{x}\|^2 + \|\mathbf{z}\|^2) \\ & \stackrel{(a)}{<} \frac{4}{3} \|\mathbf{z}\| \left(\frac{1}{2} \|\mathbf{z}\|^2 + \|\mathbf{z}\|^2 \right) \\ & = 2\|\mathbf{z}\|^3, \end{aligned} \quad (104)$$

where (a) is because $\mathbf{z} \in \mathcal{R}_0$ so that $\|\mathbf{z}\|^2 > 2\|\mathbf{x}\|^2$.

From (103) and (104), we have that

$$\begin{aligned} \|\nabla f(\mathbf{z})_{\mathcal{T}}\| & \geq \|\nabla \mathbb{E}[f(\mathbf{z})]_{\mathcal{T}}\| - \|\nabla f(\mathbf{z})_{\mathcal{T}} - \nabla \mathbb{E}[f(\mathbf{z})]_{\mathcal{T}}\| \\ & > 0, \end{aligned} \quad (105)$$

which is the desired result.

ii) For $\mathbf{z} \in \mathcal{R}_1 \subseteq \mathbb{C}^{\mathcal{T}} \setminus \mathcal{R}_0$, $\|\mathbf{z}\|$ is bounded. Thus for any constant $\delta_0 > 0$, plugging

$$\delta = \frac{\delta_0}{\sqrt{2} \max_{\mathbf{z} \in \mathcal{R}_1} \{\|\mathbf{x}\|^2 + 3\|\mathbf{z}\|^2\}}$$

into (54) of Lemma 2 yields

$$\begin{aligned} & \|\nabla^2 f(\mathbf{z})_{\mathcal{T}} - \nabla^2 \mathbb{E}[f(\mathbf{z})]_{\mathcal{T}}\| \\ & \leq \frac{\delta_0}{\max_{\mathbf{z} \in \mathcal{R}_1} \{\|\mathbf{x}\|^2 + 3\|\mathbf{z}\|^2\}} (\|\mathbf{x}\|^2 + 3\|\mathbf{z}\|^2) \\ & \leq \delta_0. \end{aligned} \quad (106)$$

This means that we can use a positive number δ_0 to bound the right-hand side of (54).

Let $\delta_0 < \frac{\delta_1}{2\|\mathbf{u}\|^2}$. Then, we have

$$\begin{aligned} & \begin{bmatrix} \mathbf{u}e^{j\phi(\mathbf{z})} \\ \bar{\mathbf{u}}e^{-j\phi(\mathbf{z})} \end{bmatrix}^* \nabla^2 f(\mathbf{z})_{\mathcal{T}} \begin{bmatrix} \mathbf{u}e^{j\phi(\mathbf{z})} \\ \bar{\mathbf{u}}e^{-j\phi(\mathbf{z})} \end{bmatrix} \\ & \leq \begin{bmatrix} \mathbf{u}e^{j\phi(\mathbf{z})} \\ \bar{\mathbf{u}}e^{-j\phi(\mathbf{z})} \end{bmatrix}^* \nabla^2 \mathbb{E}[f(\mathbf{z})]_{\mathcal{T}} \begin{bmatrix} \mathbf{u}e^{j\phi(\mathbf{z})} \\ \bar{\mathbf{u}}e^{-j\phi(\mathbf{z})} \end{bmatrix} \\ & \quad + \begin{bmatrix} \mathbf{u}e^{j\phi(\mathbf{z})} \\ \bar{\mathbf{u}}e^{-j\phi(\mathbf{z})} \end{bmatrix}^* [\nabla^2 f(\mathbf{z})_{\mathcal{T}} - \nabla^2 \mathbb{E}[f(\mathbf{z})]_{\mathcal{T}}] \begin{bmatrix} \mathbf{u}e^{j\phi(\mathbf{z})} \\ \bar{\mathbf{u}}e^{-j\phi(\mathbf{z})} \end{bmatrix} \\ & \stackrel{(106)}{\leq} \begin{bmatrix} \mathbf{u}e^{j\phi(\mathbf{z})} \\ \bar{\mathbf{u}}e^{-j\phi(\mathbf{z})} \end{bmatrix}^* \nabla^2 \mathbb{E}[f(\mathbf{z})]_{\mathcal{T}} \begin{bmatrix} \mathbf{u}e^{j\phi(\mathbf{z})} \\ \bar{\mathbf{u}}e^{-j\phi(\mathbf{z})} \end{bmatrix} + \delta_0 \cdot 2\|\mathbf{u}\|^2 \\ & \stackrel{(a)}{<} -\delta_1 + \delta_1 \\ & = 0, \end{aligned} \quad (107)$$

where (a) is because $\mathbf{z} \in \mathcal{R}_1$.

iii) For $\mathbf{z} \in \mathcal{R}_2 \subseteq \mathbb{C}^{\mathcal{T}} \setminus \mathcal{R}_0$, $\|\mathbf{z}\|$ is bounded. Thus for any constant $\delta_0 > 0$, taking

$$\delta = \frac{\delta_0}{\sqrt{2} \max_{\mathbf{z} \in \mathcal{R}_2} \{\|\mathbf{z}\|(\|\mathbf{x}\|^2 + \|\mathbf{z}\|^2)\}}$$

in (53) of Lemma 2 yields that

$$\begin{aligned} & \|\nabla f(\mathbf{z})_{\mathcal{T}} - \mathbb{E}[\nabla f(\mathbf{z})]_{\mathcal{T}}\| \\ & \leq \frac{\delta_0}{\max_{\mathbf{z} \in \mathcal{R}_2} \{\|\mathbf{z}\|(\|\mathbf{x}\|^2 + \|\mathbf{z}\|^2)\}} \|\mathbf{z}\|(\|\mathbf{x}\|^2 + \|\mathbf{z}\|^2) \\ & \leq \delta_0. \end{aligned} \quad (108)$$

This means that we can use a positive number δ_0 to bound the right-hand side of (53).

Furthermore, for any $\mathbf{z} \in \mathcal{R}_2$, we have

$$\begin{bmatrix} \mathbf{z} \\ \bar{\mathbf{z}} \end{bmatrix}^* \nabla \mathbb{E}[f(\mathbf{z})]_{\mathcal{T}} < -\delta_2. \quad (109)$$

On the other hand, using Cauchy's inequality, we have

$$\begin{bmatrix} \mathbf{z} \\ \bar{\mathbf{z}} \end{bmatrix}^* \nabla \mathbb{E}[f(\mathbf{z})]_{\mathcal{T}} \geq -\sqrt{2}\|\mathbf{z}\| \|\nabla \mathbb{E}[f(\mathbf{z})]_{\mathcal{T}}\|. \quad (110)$$

Combining (109) and (110) yields

$$\|\nabla \mathbb{E}[f(\mathbf{z})]_{\mathcal{T}}\| > \frac{\delta_2}{\sqrt{2}\|\mathbf{z}\|}. \quad (111)$$

Hence, take

$$\delta_0 < \frac{\delta_2}{2\sqrt{\|\mathbf{x}\|^2 + \|\mathbf{x}_{\mathcal{T}}\|^2}},$$

and we obtain that

$$\begin{aligned}
& \|\nabla f(\mathbf{z})_{\mathcal{T}}\| \\
& \geq \|\nabla \mathbb{E}[f(\mathbf{z})]_{\mathcal{T}}\| - \|\nabla f(\mathbf{z})_{\mathcal{T}} - \nabla \mathbb{E}[f(\mathbf{z})]_{\mathcal{T}}\| \\
& \stackrel{(111)}{>} \frac{\delta_2}{\sqrt{2}\|\mathbf{z}\|} - \delta_0 \\
& > \frac{\delta_2}{\sqrt{2}\|\mathbf{z}\|} - \frac{\delta_2}{2\sqrt{\|\mathbf{x}\|^2 + \|\mathbf{x}_{\mathcal{T}}\|^2}} \\
& \stackrel{(a)}{\geq} 0, \tag{112}
\end{aligned}$$

where (a) follows from the fact that $\mathbf{z} \in \mathbb{C}^{\mathcal{T}} \setminus \mathcal{R}_0$ so that $\|\mathbf{z}\|^2 \leq 2(\|\mathbf{x}\|^2 + \|\mathbf{x}_{\mathcal{T}}\|^2)$.

iv) For $\mathbf{z} \in \mathcal{R}_3 \subseteq \mathbb{C}^{\mathcal{T}} \setminus \mathcal{R}_0$, with the same method as (108), we have

$$\|\nabla f(\mathbf{z})_{\mathcal{T}} - \mathbb{E}[\nabla f(\mathbf{z})]_{\mathcal{T}}\| \leq \delta_0. \tag{113}$$

Furthermore, for any $\mathbf{z} \in \mathcal{R}_3$, we have

$$\left[\begin{array}{c} \mathbf{z} - \mathbf{u}e^{j\phi} \\ \bar{\mathbf{z}} - \bar{\mathbf{u}}e^{-j\phi} \end{array} \right]^* \nabla \mathbb{E}[f(\mathbf{z})]_{\mathcal{T}} > \delta_3, \tag{114}$$

where ϕ is simplified for $\phi(\mathbf{z})$. On the other hand, using Cauchy's inequality, we have

$$\begin{aligned}
& \sqrt{2}\|\mathbf{z} - \mathbf{u}e^{j\phi}\| \|\nabla \mathbb{E}[f(\mathbf{z})]_{\mathcal{T}}\| \\
& \geq \left[\begin{array}{c} \mathbf{z} - \mathbf{u}e^{j\phi} \\ \bar{\mathbf{z}} - \bar{\mathbf{u}}e^{-j\phi} \end{array} \right]^* \nabla \mathbb{E}[f(\mathbf{z})]_{\mathcal{T}}. \tag{115}
\end{aligned}$$

Combining (114) and (115) yields

$$\|\nabla \mathbb{E}[f(\mathbf{z})]_{\mathcal{T}}\| > \frac{\delta_3}{\sqrt{2}\|\mathbf{z} - \mathbf{u}e^{j\phi(\mathbf{z})}\|}. \tag{116}$$

Hence, take

$$\delta_0 < \frac{\delta_3}{3\sqrt{\|\mathbf{x}\|^2 + \|\mathbf{x}_{\mathcal{T}}\|^2}},$$

and we have

$$\begin{aligned}
& \|\nabla f(\mathbf{z})_{\mathcal{T}}\| \\
& \geq \|\nabla \mathbb{E}[f(\mathbf{z})]_{\mathcal{T}}\| - \|\nabla f(\mathbf{z})_{\mathcal{T}} - \nabla \mathbb{E}[f(\mathbf{z})]_{\mathcal{T}}\| \\
& \stackrel{(116)}{>} \frac{\delta_3}{\sqrt{2}\|\mathbf{z} - \mathbf{u}e^{j\phi}\|} - \delta_0 \\
& > \frac{\delta_3}{\sqrt{2}\|\mathbf{z} - \mathbf{u}e^{j\phi}\|} - \frac{\delta_3}{3\sqrt{\|\mathbf{x}\|^2 + \|\mathbf{x}_{\mathcal{T}}\|^2}} \\
& \geq \frac{\delta_3}{\sqrt{2}(\|\mathbf{z}\| + \|\mathbf{u}\|)} - \frac{\delta_3}{3\sqrt{\|\mathbf{x}\|^2 + \|\mathbf{x}_{\mathcal{T}}\|^2}} \\
& \stackrel{(a)}{\geq} \frac{\delta_3}{\sqrt{2}\left(\|\mathbf{z}\| + \sqrt{(\|\mathbf{x}\|^2 + \|\mathbf{x}_{\mathcal{T}}\|^2)/2}\right)} \\
& \quad - \frac{\delta_3}{3\sqrt{\|\mathbf{x}\|^2 + \|\mathbf{x}_{\mathcal{T}}\|^2}} \\
& \stackrel{(b)}{\geq} 0, \tag{117}
\end{aligned}$$

where (a) is because $\mathbf{u} = \lambda_{\mathcal{T}}\mathbf{x}_{\mathcal{T}}$ and (b) is from the fact that $\mathbf{z} \in \mathbb{C}^{\mathcal{T}} \setminus \mathcal{R}_0$ so that $\|\mathbf{z}\|^2 \leq 2(\|\mathbf{x}\|^2 + \|\mathbf{x}_{\mathcal{T}}\|^2)$.

By collecting the results in (105), (107), (112) and (117), we complete the proof of (60).

Part 2: Now, we proceed to the second part of proof for Proposition 2. To the end, it suffices to show that $\mathbb{C}^{\mathcal{T}} \subseteq \cup_{i=0}^4 \mathcal{R}_i$.

First, define three functions as below.

$$\begin{aligned}
g_1(\mathbf{z}) & \doteq \left[\begin{array}{c} \mathbf{u}e^{j\phi(\mathbf{z})} \\ \bar{\mathbf{u}}e^{-j\phi(\mathbf{z})} \end{array} \right]^* \nabla^2 \mathbb{E}[f(\mathbf{z})]_{\mathcal{T}} \left[\begin{array}{c} \mathbf{u}e^{j\phi(\mathbf{z})} \\ \bar{\mathbf{u}}e^{-j\phi(\mathbf{z})} \end{array} \right] \\
& = (\|\mathbf{x}\|^2 + \|\mathbf{x}_{\mathcal{T}}\|^2) \\
& \quad \times \left(4 \frac{|\mathbf{x}_{\mathcal{T}}^* \mathbf{z}|^2}{\|\mathbf{x}_{\mathcal{T}}\|^2} + 2\|\mathbf{z}\|^2 - \|\mathbf{x}\|^2 - \|\mathbf{x}_{\mathcal{T}}\|^2 \right), \tag{118}
\end{aligned}$$

$$\begin{aligned}
g_2(\mathbf{z}) & \doteq \left[\begin{array}{c} \mathbf{z} \\ \bar{\mathbf{z}} \end{array} \right]^* \nabla \mathbb{E}[f(\mathbf{z})]_{\mathcal{T}} \\
& = 2(2\|\mathbf{z}\|^2 - \|\mathbf{x}\|^2) \|\mathbf{z}\|^2 - 2|\mathbf{x}_{\mathcal{T}}^* \mathbf{z}|^2 \tag{119}
\end{aligned}$$

$$\begin{aligned}
g_3(\mathbf{z}) & \doteq \left[\begin{array}{c} \mathbf{z} - \mathbf{u}e^{j\phi(\mathbf{z})} \\ \bar{\mathbf{z}} - \bar{\mathbf{u}}e^{-j\phi(\mathbf{z})} \end{array} \right]^* \nabla \mathbb{E}[f(\mathbf{z})]_{\mathcal{T}} \\
& = 2((2\|\mathbf{z}\|^2 - \|\mathbf{x}\|^2)(\|\mathbf{z}\|^2 - |\lambda_{\mathcal{T}}| |\mathbf{x}_{\mathcal{T}}^* \mathbf{z}|) \\
& \quad - (|\mathbf{x}_{\mathcal{T}}^* \mathbf{z}| - |\lambda_{\mathcal{T}}| \|\mathbf{x}_{\mathcal{T}}\|^2) |\mathbf{x}_{\mathcal{T}}^* \mathbf{z}|), \tag{120}
\end{aligned}$$

where $|\lambda_{\mathcal{T}}| = \sqrt{\frac{\|\mathbf{x}\|^2 + \|\mathbf{x}_{\mathcal{T}}\|^2}{2\|\mathbf{x}_{\mathcal{T}}\|^2}}$.

Next, we divide $\mathbb{C}^{\mathcal{T}}$ into six disjointed regions: \mathcal{R}_a , \mathcal{R}_b , \mathcal{R}_c , \mathcal{R}_d , \mathcal{R}_e and \mathcal{R}_0 .

$$i) \mathcal{R}_a \doteq \left\{ \mathbf{z} \in \mathbb{C}^{\mathcal{T}} : \|\mathbf{z}\|^2 \leq \frac{\|\mathbf{x}\|^2 - \sqrt{\|\mathbf{x}\|^4 - 4\delta_2}}{4} \right\}.$$

When $\mathbf{z} \in \mathcal{R}_a$, we have

$$g_1(\mathbf{z}) \leq (\|\mathbf{x}\|^2 + \|\mathbf{x}_{\mathcal{T}}\|^2) (6\|\mathbf{z}\|^2 - \|\mathbf{x}\|^2 - \|\mathbf{x}_{\mathcal{T}}\|^2). \tag{121}$$

If we can show that

$$(\|\mathbf{x}\|^2 + \|\mathbf{x}_{\mathcal{T}}\|^2) (6\|\mathbf{z}\|^2 - \|\mathbf{x}\|^2 - \|\mathbf{x}_{\mathcal{T}}\|^2) < -\delta_1 \tag{122}$$

holds for any $\mathbf{z} \in \mathcal{R}_a$, then we can claim that $\mathcal{R}_a \subseteq \mathcal{R}_1$. Note that (122) is equivalent to

$$\|\mathbf{z}\|^2 < \frac{(\|\mathbf{x}\|^2 + \|\mathbf{x}_{\mathcal{T}}\|^2)^2 - \delta_1}{6(\|\mathbf{x}\|^2 + \|\mathbf{x}_{\mathcal{T}}\|^2)}, \tag{123}$$

and

$$\lim_{\delta_2 \rightarrow 0^+} \frac{\|\mathbf{x}\|^2 - \sqrt{\|\mathbf{x}\|^4 - 4\delta_2}}{4} = 0$$

Thus, for any fixed positive $\delta_1 < (\|\mathbf{x}\|^2 + \|\mathbf{x}_{\mathcal{T}}\|^2)^2$, there always exists a small $\delta_2 > 0$ such that (123) holds for any $\mathbf{z} \in \mathcal{R}_a$, and thus $g_1(\mathbf{z}) < -\delta_1$. Therefore, we can conclude that for any fixed positive $\delta_1 < (\|\mathbf{x}\|^2 + \|\mathbf{x}_{\mathcal{T}}\|^2)^2$, there exists a small $\delta_2 > 0$ such that $\mathcal{R}_a \subseteq \mathcal{R}_1$.

$$ii) \mathcal{R}_b \doteq \left\{ \mathbf{z} \in \mathbb{C}^{\mathcal{T}} : \frac{\|\mathbf{x}\|^2 - \sqrt{\|\mathbf{x}\|^4 - 4\delta_2}}{4} < \|\mathbf{z}\|^2 < \frac{\|\mathbf{x}\|^2 + \sqrt{\|\mathbf{x}\|^4 - 4\delta_2}}{4} \right\}.$$

When $\mathbf{z} \in \mathcal{R}_b$, it is easy to verify that

$$\begin{aligned}
g_2(\mathbf{z}) & = 2(2\|\mathbf{z}\|^2 - \|\mathbf{x}\|^2) \|\mathbf{z}\|^2 - 2|\mathbf{x}_{\mathcal{T}}^* \mathbf{z}|^2 \\
& \leq 2(2\|\mathbf{z}\|^2 - \|\mathbf{x}\|^2) \|\mathbf{z}\|^2 \\
& \leq -\delta_2. \tag{124}
\end{aligned}$$

The last inequality is because we can treat the term as a second-order polynomial of $\|\mathbf{z}\|^2$. This implies that $\mathbf{z} \in \mathcal{R}_2$, and furthermore, $\mathcal{R}_b \subseteq \mathcal{R}_2$.

$$\text{iii) } \mathcal{R}_c \doteq \left\{ \mathbf{z} \in \mathbb{C}^{\mathcal{T}} : \frac{\|\mathbf{x}\|^2 + \sqrt{\|\mathbf{x}\|^4 - 4\delta_2}}{4} \leq \|\mathbf{z}\|^2 < \frac{1}{2}\|\mathbf{x}\|^2 \text{ and } |\mathbf{x}_{\mathcal{T}}^* \mathbf{z}| < \frac{\|\mathbf{x}_{\mathcal{T}}\|}{2} \sqrt{\|\mathbf{x}_{\mathcal{T}}\|^2 - \frac{\delta_1}{\|\mathbf{x}\|^2 + \|\mathbf{x}_{\mathcal{T}}\|^2}} \right\}.$$

It is easy to verify that for any $\mathbf{z} \in \mathcal{R}_c$,

$$\begin{aligned} g_1(\mathbf{z}) &= \left(\|\mathbf{x}\|^2 + \|\mathbf{x}_{\mathcal{T}}\|^2 \right) \\ &\quad \times \left(4 \frac{|\mathbf{x}_{\mathcal{T}}^* \mathbf{z}|^2}{\|\mathbf{x}_{\mathcal{T}}\|^2} + 2\|\mathbf{z}\|^2 - \|\mathbf{x}\|^2 - \|\mathbf{x}_{\mathcal{T}}\|^2 \right) \\ &\leq \left(\|\mathbf{x}\|^2 + \|\mathbf{x}_{\mathcal{T}}\|^2 \right) \left(4 \times \frac{|\mathbf{x}_{\mathcal{T}}^* \mathbf{z}|^2}{\|\mathbf{x}_{\mathcal{T}}\|^2} - \|\mathbf{x}_{\mathcal{T}}\|^2 \right) \\ &< -\delta_1. \end{aligned} \quad (125)$$

This implies that $\mathbf{z} \in \mathcal{R}_1$, and furthermore, $\mathcal{R}_c \subseteq \mathcal{R}_1$.

$$\text{iv) } \mathcal{R}_d \doteq \left\{ \mathbf{z} \in \mathbb{C}^{\mathcal{T}} : \frac{\|\mathbf{x}\|^2 + \sqrt{\|\mathbf{x}\|^4 - 4\delta_2}}{4} \leq \|\mathbf{z}\|^2 < \frac{1}{2}\|\mathbf{x}\|^2 \text{ and } |\mathbf{x}_{\mathcal{T}}^* \mathbf{z}| \geq \frac{\|\mathbf{x}_{\mathcal{T}}\|}{2} \sqrt{\|\mathbf{x}_{\mathcal{T}}\|^2 - \frac{\delta_1}{\|\mathbf{x}\|^2 + \|\mathbf{x}_{\mathcal{T}}\|^2}} \right\}.$$

Computing this directly, we obtain

$$\begin{aligned} g_2(\mathbf{z}) &= 2(2\|\mathbf{z}\|^2 - \|\mathbf{x}\|^2)\|\mathbf{z}\|^2 - 2|\mathbf{x}_{\mathcal{T}}^* \mathbf{z}|^2 \\ &\leq -2|\mathbf{x}_{\mathcal{T}}^* \mathbf{z}|^2 \\ &\leq -\frac{\|\mathbf{x}_{\mathcal{T}}\|^2}{2} \left(\|\mathbf{x}_{\mathcal{T}}\|^2 - \frac{\delta_1}{\|\mathbf{x}\|^2 + \|\mathbf{x}_{\mathcal{T}}\|^2} \right). \end{aligned} \quad (126)$$

Then, if we let

$$\delta_2 < \frac{\|\mathbf{x}_{\mathcal{T}}\|^2}{2} \left(\|\mathbf{x}_{\mathcal{T}}\|^2 - \frac{\delta_1}{\|\mathbf{x}\|^2 + \|\mathbf{x}_{\mathcal{T}}\|^2} \right), \quad (127)$$

then we can claim that $g_2(\mathbf{z}) < -\delta_2$ holds for any $\mathbf{z} \in \mathcal{R}_d$, and thus $\mathcal{R}_d \subseteq \mathcal{R}_2$. Since $\delta_2 > 0$, thus, for any fixed positive $\delta_1 < \|\mathbf{x}_{\mathcal{T}}\|^2(\|\mathbf{x}\|^2 + \|\mathbf{x}_{\mathcal{T}}\|^2)$, there exists a small $\delta_2 > 0$ such that (127) holds and $\mathcal{R}_d \subseteq \mathcal{R}_2$.

$$\text{v) } \mathcal{R}_e \doteq \left\{ \mathbf{z} \in \mathbb{C}^{\mathcal{T}} : \frac{1}{2}\|\mathbf{x}\|^2 \leq \|\mathbf{z}\|^2 \leq 2(\|\mathbf{x}\|^2 + \|\mathbf{x}_{\mathcal{T}}\|^2) \right\}.$$

We have

$$\begin{aligned} g_3(\mathbf{z}) &= 2 \left((2\|\mathbf{z}\|^2 - \|\mathbf{x}\|^2) (\|\mathbf{z}\|^2 - |\lambda_{\mathcal{T}}| |\mathbf{x}_{\mathcal{T}}^* \mathbf{z}|) \right. \\ &\quad \left. - \left(|\mathbf{x}_{\mathcal{T}}^* \mathbf{z}| - |\lambda_{\mathcal{T}}| \|\mathbf{x}_{\mathcal{T}}\|^2 \right) |\mathbf{x}_{\mathcal{T}}^* \mathbf{z}| \right). \end{aligned} \quad (128)$$

Note that \mathbf{z} can be decomposed by two independent components: i) the norm $\|\mathbf{z}\|$ and ii) the direction $\frac{\mathbf{z}}{\|\mathbf{z}\|}$. Hence, when $\|\mathbf{z}\|$ is fixed, $g_3(\mathbf{z})$ is a second-order polynomial in $|\mathbf{x}_{\mathcal{T}}^* \mathbf{z}|$ with coefficients of the second-order terms smaller than 0. Therefore, $g_3(\mathbf{z})$ achieves the minimum when

$$|\mathbf{x}_{\mathcal{T}}^* \mathbf{z}| = 0 \text{ or } |\mathbf{x}_{\mathcal{T}}^* \mathbf{z}| = \|\mathbf{x}_{\mathcal{T}}\| \|\mathbf{z}\|. \quad (129)$$

a) **Case 1:** $|\mathbf{x}_{\mathcal{T}}^* \mathbf{z}| = 0$.

$$g_3(\mathbf{z}) = 2 \left((2\|\mathbf{z}\|^2 - \|\mathbf{x}\|^2) \|\mathbf{z}\|^2 \right) \geq 0. \quad (130)$$

In this case, $g_3(\mathbf{z}) = 0$ if and only if $\|\mathbf{z}\|^2 = \frac{1}{2}\|\mathbf{x}\|^2$. But when this equality holds, $g_1(\mathbf{z}) = -\|\mathbf{x}_{\mathcal{T}}\|^2(\|\mathbf{x}\|^2 + \|\mathbf{x}_{\mathcal{T}}\|^2) < 0$.

b) **Case 2:** $|\mathbf{x}_{\mathcal{T}}^* \mathbf{z}| = \|\mathbf{x}_{\mathcal{T}}\| \|\mathbf{z}\|$.

$$\begin{aligned} g_3(\mathbf{z}) &= 2 \left((2\|\mathbf{z}\|^2 - \|\mathbf{x}\|^2) (\|\mathbf{z}\|^2 - |\lambda_{\mathcal{T}}| \|\mathbf{x}_{\mathcal{T}}\| \|\mathbf{z}\|) \right. \\ &\quad \left. - \left(\|\mathbf{x}_{\mathcal{T}}\| \|\mathbf{z}\| - |\lambda_{\mathcal{T}}| \|\mathbf{x}_{\mathcal{T}}\|^2 \right) \|\mathbf{x}_{\mathcal{T}}\| \|\mathbf{z}\| \right) \\ &= \|\mathbf{z}\| \left(2\|\mathbf{z}\|^2 - \|\mathbf{x}\|^2 - \|\mathbf{x}_{\mathcal{T}}\|^2 \right) \\ &\quad \times \left(\|\mathbf{z}\| - \sqrt{\frac{\|\mathbf{x}\|^2 + \|\mathbf{x}_{\mathcal{T}}\|^2}{2}} \right) \\ &\geq 0. \end{aligned} \quad (131)$$

It is trivial to see that in this case $g_3(\mathbf{z}) = 0$ if and only if $\mathbf{z} = \lambda_{\mathcal{T}} \mathbf{x}_{\mathcal{T}}$.

In conclusion, $g_3(\mathbf{z})$ is always nonnegative. Then, for any fixed positive $\delta_1 < \|\mathbf{x}_{\mathcal{T}}\|^2(\|\mathbf{x}\|^2 + \|\mathbf{x}_{\mathcal{T}}\|^2)$ and δ_4 , define

$$K(\delta_1, \delta_4) \doteq \inf_{\mathbf{z} \in \mathcal{R}_e \setminus (\mathcal{R}_1 \cup \mathcal{R}_4)} g_3(\mathbf{z}) > 0. \quad (132)$$

Let $0 < \delta_3 < K(\delta_1, \delta_4)$. Then, for any $\mathbf{z} \in \mathcal{R}_e$ satisfying $g_3(\mathbf{z}) \leq \delta_3$, we have $\mathbf{z} \in \mathcal{R}_1 \cup \mathcal{R}_4$. When $g_3(\mathbf{z}) > \delta_3$, $\mathbf{z} \in \mathcal{R}_3$. Consequently, $\mathcal{R}_e \subseteq \mathcal{R}_1 \cup \mathcal{R}_3 \cup \mathcal{R}_4$.

Finally, we obtain that for any $\delta_1, \delta_4 > 0$, there exist $\delta_2, \delta_3 > 0$ such that

$$\mathbb{C}^{\mathcal{T}} = \mathcal{R}_a \cup \mathcal{R}_b \cup \mathcal{R}_c \cup \mathcal{R}_d \cup \mathcal{R}_e \cup \mathcal{R}_0 \subseteq \bigcup_{i=0}^4 \mathcal{R}_i. \quad (133)$$

The proof is thus complete. \square

C. Proof of Proposition 3

Proof. When $\mathcal{T} \supseteq \text{supp}(\mathbf{x})$, we know from Proposition 2 that the solution to (19) is a zero point of $\nabla f(\mathbf{z})_{\mathcal{T}}$ in \mathcal{R}_4 . Thus, to prove Proposition 3 (i.e., to prove that the solution to (19) is exactly \mathbf{x} up to a global phase), it suffices to show that all the zero points of $\nabla f(\mathbf{z})_{\mathcal{T}}$ in \mathcal{R}_4 are exactly \mathbf{x} up to a global phase. In the following, we shall show this fact by using some results of [1].

By taking

$$\delta_4 \leq \frac{1}{\sqrt{7}} \|\mathbf{x}\|,$$

the result in [1, Proposition 2.4] implies the restricted strong convexity of $f(\mathbf{z})$ in \mathcal{R}_4 . That is, when $m \geq Ck \log k$, it holds with probability exceeding $1 - cm^{-1}$ that

$$\left[\frac{\mathbf{g}(\mathbf{z})}{\|\mathbf{g}(\mathbf{z})\|} \right]^* \nabla^2 f(\mathbf{z})_{\mathcal{T}} \left[\frac{\mathbf{g}(\mathbf{z})}{\|\mathbf{g}(\mathbf{z})\|} \right] \geq \frac{1}{4} \|\mathbf{x}\|^2, \quad \forall \mathbf{z} \in \mathcal{R}_4, \quad (134)$$

where

$$\mathbf{g}(\mathbf{z}) \doteq \begin{cases} \frac{\mathbf{z} - \mathbf{x} e^{j\phi(\mathbf{z})}}{\|\mathbf{z} - \mathbf{x} e^{j\phi(\mathbf{z})}\|} & \text{if } \text{dist}(\mathbf{z}, \mathbf{x}) \neq 0, \\ \{\mathbf{p} \in \{\mathbf{p} : \Im(\mathbf{p}^* \mathbf{z}) = 0, \|\mathbf{p}\| = 1\}\} & \text{otherwise,} \end{cases}$$

$\phi(\mathbf{z}) = \arg \min_{\phi \in [0, 2\pi)} \|\mathbf{z} - \mathbf{x} e^{j\phi}\|$ and $\Im(\mathbf{p}^* \mathbf{z})$ is the imaginary part of $\mathbf{p}^* \mathbf{z}$.

For any $\mathbf{z} \in \mathcal{R}_4$, if $\text{dist}(\mathbf{z}, \mathbf{x}) \neq 0$, applying the same integral form of Taylor's theorem as in [1, Theorem 2.2], together with the restricted strong convexity of $f(\mathbf{z})$ obtained above, yields

$$\|\nabla f(\mathbf{z})_{\mathcal{T}}\| \neq 0. \quad (135)$$

In other words, $\mathbf{z} \in \mathcal{R}_4$ must not be a zero point of $\nabla f(\mathbf{z})_{\mathcal{T}}$ if $\text{dist}(\mathbf{z}, \mathbf{x}) \neq 0$. This in turn implies that

$$\text{dist}(\mathbf{z}, \mathbf{x}) = 0$$

whenever $\mathbf{z} \in \mathcal{R}_4$ satisfies $\nabla f(\mathbf{z})_{\mathcal{T}} = \mathbf{0}$. The proof is thus complete. \square

REFERENCES

- [1] J. Sun, Q. Qu, and J. Wright, "A geometric analysis of phase retrieval," *Found. Comput. Math.*, vol. 18, no. 5, pp. 1615–3375, Oct. 2018.
- [2] R. P. Millane, "Phase retrieval in crystallography and optics," *J. Opt. Soc. Amer. A*, vol. 7, no. 3, pp. 394–411, Mar. 1990.
- [3] Y. Shechtman, Y. C. Eldar, O. Cohen, H. N. Chapman, J. Miao, and M. Segev, "Phase retrieval with application to optical imaging: A contemporary overview," *IEEE Signal Process. Mag.*, vol. 32, no. 3, pp. 87–109, 2015.
- [4] A. Walther, "The question of phase retrieval in optics," *Opt. Acta (Lond)*, vol. 10, no. 1, pp. 41–49, 1963.
- [5] R. W. Harrison, "Phase problem in crystallography," *J. Opt. Soc. Amer. A*, vol. 10, no. 5, pp. 1046–1055, May 1993.
- [6] J. Dainty and J. Fienup, "Phase retrieval and image reconstruction for astronomy," *Image Recovery: Theory Appl.*, vol. 13, Jan. 1987.
- [7] K. Jaganathan, Y. C. Eldar, and B. Hassibi, "Phase retrieval: An overview of recent developments," *arXiv preprint arXiv:1510.07713*, 2015.
- [8] R. W. Gerchberg, "A practical algorithm for the determination of phase from image and diffraction plane pictures," *Optik*, vol. 35, pp. 237–246, 1972.
- [9] J. Fienup, "Reconstruction of an object from modulus of its fourier transform," *Opt. Lett.*, vol. 3, pp. 27–9, Aug. 1978.
- [10] H. H. Bauschke, P. L. Combettes, and D. R. Luke, "Phase retrieval, error reduction algorithm, and fienu variants: a view from convex optimization," *J. Opt. Soc. Amer. A*, vol. 19, no. 7, pp. 1334–1345, Jul. 2002.
- [11] E. J. Candès, T. Strohmer, and V. Voroninski, "Phaselift: Exact and stable signal recovery from magnitude measurements via convex programming," *Commun. Pure Appl. Math.*, vol. 66, no. 8, pp. 1241–1274, 2013.
- [12] I. Waldspurger, A. d'Aspremont, and S. Mallat, "Phase recovery, maxcut and complex semidefinite programming," *Math. Program.*, vol. 149, no. 1, pp. 47–81, 2015.
- [13] T. Goldstein and C. Studer, "Phasemax: Convex phase retrieval via basis pursuit," *IEEE Trans. Inf. Theory*, vol. 64, no. 4, pp. 2675–2689, 2018.
- [14] B. Wang, J. Fang, H. Duan, and H. Li, "Phaseequal: Convex phase retrieval via alternating direction method of multipliers," *IEEE Trans. Signal Process.*, vol. 68, pp. 1274–1285, 2020.
- [15] E. J. Candès, X. Li, and M. Soltanolkotabi, "Phase retrieval via wirtinger flow: Theory and algorithms," *IEEE Trans. Inf. Theory*, vol. 61, no. 4, pp. 1985–2007, 2015.
- [16] H. Zhang and Y. Liang, "Reshaped wirtinger flow for solving quadratic system of equations," *Adv. Neural Inf. Process. Syst.*, vol. 29, pp. 2622–2630, 2016.
- [17] Y. Chen and E. Candès, "Solving random quadratic systems of equations is nearly as easy as solving linear systems," *Commun. Pure Appl. Math.*, vol. 70, May 2015.
- [18] Y. Xia and Z. Xu, "The recovery of complex sparse signals from few phaseless measurements," *Appl. Comput. Harmon. Anal.*, vol. 50, pp. 1–15, 2021.
- [19] Y. Shechtman, A. Beck, and Y. C. Eldar, "Gespar: Efficient phase retrieval of sparse signals," *IEEE Trans. Signal Process.*, vol. 62, no. 4, pp. 928–938, 2014.
- [20] G. Wang, L. Zhang, G. B. Giannakis, M. Akçakaya, and J. Chen, "Sparse phase retrieval via truncated amplitude flow," *IEEE Trans. Signal Process.*, vol. 66, no. 2, pp. 479–491, 2018.
- [21] Z. Yuan, H. Wang, and Q. Wang, "Phase retrieval via sparse wirtinger flow," *J. Comput.*, vol. 355, pp. 162–173, 2019.
- [22] Y. C. Eldar and S. Mendelson, "Phase retrieval: Stability and recovery guarantees," *Appl. Comput. Harmon. Anal.*, vol. 36, no. 3, pp. 473–494, 2014.
- [23] L. V. Truong and J. Scarlett, "Support recovery in the phase retrieval model: Information-theoretic fundamental limit," *IEEE Trans. Inf. Theory*, vol. 66, no. 12, pp. 7887–7910, 2020.
- [24] F. Wu and P. Rebeschini, "Hadamard wirtinger flow for sparse phase retrieval," in *Int. Conf. Artif. Intell. Statist.*, 2021, pp. 982–990.
- [25] Z. Liu, S. Ghosh, and J. Scarlett, "Towards sample-optimal compressive phase retrieval with sparse and generative priors," *Adv. Neural Inf. Process. Syst.*, vol. 34, 2021.
- [26] H. Zou, T. Hastie, and R. Tibshirani, "Sparse principal component analysis," *J. Comput. Graph. Statist.*, vol. 15, no. 2, pp. 265–286, 2006.
- [27] Q. Berthet and P. Rigollet, "Complexity theoretic lower bounds for sparse principal component detection," in *Proc. 26th Annu. Conf. Learn. Theory*, S. Shalev-Shwartz and I. Steinwart, Eds., vol. 30, Jun. 2013, pp. 1046–1066.
- [28] K. Kreutz-Delgado, "The complex gradient operator and the cr-calculus," *arXiv preprint arXiv:0906.4835*, 2009.
- [29] C. Jin, R. Ge, P. Netrapalli, S. M. Kakade, and M. I. Jordan, "How to escape saddle points efficiently," in *Proc. 34th Int. Conf. Mach. Learn.*, vol. 70, Aug. 2017, pp. 1724–1732.
- [30] J. Barzilai and J. Borwein, "Two-point step size gradient methods," *IMA J. Numer. Anal.*, vol. 8, pp. 141–148, Jan. 1988.
- [31] J. A. Tropp and A. C. Gilbert, "Signal recovery from random measurements via orthogonal matching pursuit," *IEEE Trans. Inf. Theory*, vol. 53, no. 12, pp. 4655–4666, 2007.
- [32] M. A. Davenport and M. B. Wakin, "Analysis of orthogonal matching pursuit using the restricted isometry property," *IEEE Trans. Inf. Theory*, vol. 56, no. 9, pp. 4395–4401, 2010.
- [33] J. Wang, S. Kwon, and B. Shim, "Generalized orthogonal matching pursuit," *IEEE Trans. Signal Process.*, vol. 60, no. 12, pp. 6202–6216, 2012.
- [34] E. D. Livshitz and V. N. Temlyakov, "Sparse approximation and recovery by greedy algorithms," *IEEE Trans. Inf. Theory*, vol. 60, no. 7, pp. 3989–4000, Jul. 2014.
- [35] W. Dai and O. Milenkovic, "Subspace pursuit for compressive sensing signal reconstruction," *IEEE Trans. Inf. Theory*, vol. 55, no. 5, pp. 2230–2249, 2009.
- [36] D. Needell and J. Tropp, "Cosamp: Iterative signal recovery from incomplete and inaccurate samples," *Appl. Comput. Harmon. Anal.*, vol. 26, no. 3, pp. 301–321, 2009.
- [37] M. J. Wainwright, *High-Dimensional Statistics: A Non-Asymptotic Viewpoint*. Cambridge University Press, 2019.
- [38] G. L. Stuber, *Principles of Mobile Communication*. Kluwer Academic Publishers, 1996.
- [39] P. Netrapalli, P. Jain, and S. Sanghavi, "Phase retrieval using alternating minimization," *IEEE Trans. Signal Process.*, vol. 63, no. 18, pp. 4814–4826, 2015.
- [40] Z. Li, J.-F. Cai, and K. Wei, "Toward the optimal construction of a loss function without spurious local minima for solving quadratic equations," *IEEE Trans. Inf. Theory*, vol. 66, no. 5, pp. 3242–3260, 2020.
- [41] G. Wang, G. B. Giannakis, and Y. C. Eldar, "Solving systems of random quadratic equations via truncated amplitude flow," *IEEE Trans. Inf. Theory*, vol. 64, no. 2, pp. 773–794, 2018.
- [42] R. Chandra, Z. Zhong, J. Hontz, V. McCulloch, C. Studer, and T. Goldstein, "Phasepack: A phase retrieval library," *Asilomar Conf. Signals, Syst., and Computers*, 2017.
- [43] F. Wu and P. Rebeschini, "Nearly minimax-optimal rates for noisy sparse phase retrieval via early-stopped mirror descent," *arXiv Preprint, arXiv:2105.03678*, 2021.
- [44] H. Li and S. Li, "Phase retrieval from Fourier measurements with masks," *Inverse Problems Imag.*, vol. 15, no. 5, pp. 1051–1075, 2021.